Chemical Geology 629 (2023) 121473

Contents lists available at ScienceDirect

Chemical Geology

journal homepage: www.elsevier.com/locate/chemgeo

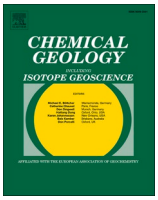

Silicic volcanic rocks, a main regional source of geogenic arsenic in waters: Insights from the Altiplano-Puna plateau, Central Andes

Jesica Murray [a,b,*], Silvina Guzmán [a,c], Joseline Tapia [d,e,f], D. Kirk Nordstrom [g]

[a] Instituto de Bio y Geociencias del NOA (IBIGEO), Universidad Nacional de Salta - CONICET, Rosario de Lerma, Salta, Argentina
[b] Institut Terre et Environnement de Strasbourg (ITES), Université de Strasbourg, CNRS, UMR 7063, Strasbourg, France
[c] National Institute of Oceanography and Applied Geophysics (OGS), Sgonico, Italy
[d] Departamento de Ciencias Geológicas, Universidad Católica del Norte, Antofagasta, Chile
[e] Centro de Estudio del Agua del Desierto (CEITSAZA), Universidad Católica del Norte, Antofagasta, Chile
[f] Instituto Milenio en Riesgo Volcánico CKELAR, Chile
[g] United States Geological Survey (USGS), Boulder, CO, USA

ARTICLE INFO

Editor: Karen Johannesson

Keywords:
Geogenic arsenic
Silicic volcanic rocks
Rhyolites
Volcanic ash
Water

ABSTRACT

Volcanic rocks are a common, worldwide source of geogenic arsenic (As) that can affect water quality detrimentally. Nonetheless, variations of As concentration within different types of volcanic rocks and questions related to the original source of As in magma are not yet fully understood. We compiled published As data from the abundant Cenozoic volcanic rocks of the Altiplano-Puna plateau, considered the main source of As for waters in the region. These data indicates that volcanic rocks in the Altiplano-Puna have a mean As concentration of 9.1 mg/kg, which is almost 2 times higher than the upper continental crust. Arsenic increases within the more silicic compositions such as dacites and rhyolites as well as from mafic monogenetic volcanic edifices to stratovolcanoes of intermediate composition, silicic calderas and ignimbrite fields. The rate and composition of crustal assimilation by the magmas (enhanced by the crustal thickness up to >70 km) strongly influence the As concentration in volcanic rocks. The assimilation of argillaceous shale-type sediments represents the most important source of As in the magmas. The eruption dynamics has an enormous effect on As concentration. The higher the explosivity of an eruption, the higher the amount of ash that will be formed. Arsenic can be sorb onto ash particles so that fall deposits produced during explosive volcanic eruptions are prone to high As concentrations. Large volume ignimbrites formed after caldera collapses in the Altiplano-Puna are often the result of sustained explosive eruptions related to low, dense pyroclastic fountaining eruptions where highly concentrated pyroclastic density currents (PDC, flowing pyroclastic mixtures of particles and gas) are able to maintain high temperatures for long periods. Then As released from volatiles may remain for longer time in the emplacing PDC and can be sorbed onto ash particles, resulting in deposits with a higher As concentration. Post eruption hydrothermal alteration and sulfide mineralization produce As enrichment up to 100 times in the volcanic rocks (957 mg/kg) of the region, but can be very heterogeneous. Volcanism and its related products are the main source of As in the region. Once As is released from the volcanic sources, the semiarid climate, the occurrence of Na-HCO_3 water types, and alkaline pH further enhance As concentrations in surface water and groundwater.

1. Introduction

Volcanic deposits and especially those containing abundant fine ash rich in glass shards are among the most common, worldwide sources of geogenic arsenic (As) in waters (Nordstrom, 2002; Bowell et al., 2014; Plant et al., 2014). The presence of inorganic As in drinking water with levels higher than the recommended limit (> 10 μg/L) presents a worldwide health concern (World Health Organization (WHO), 2022). Inorganic As is carcinogenic, mutagenic, and teratogenic for humans and increases the risks of developing several types of severe diseases from chronic exposure (IRIS (Integrated Risk Information System), 1991). At the global scale, volcanism on Earth is not randomly distributed; rather there exists a clear spatial and geochemical correlation between tectonic activity and magmatism, subduction borders, and rift

* Corresponding author at: Instituto de Bio y Geo Ciencias del NOA, Universidad Nacional de Salta - CONICET, Rosario de Lerma, Salta, Argentina.
E-mail address: murray.jesica@conicet.gov.ar (J. Murray).

https://doi.org/10.1016/j.chemgeo.2023.121473
Received 4 October 2022; Received in revised form 22 February 2023; Accepted 5 April 2023
Available online 12 April 2023

margins (e.g. LaFemina, 2015). In Fig. 1 we present data on As in volcanic rocks associated to these type of margins obtained after the GEOROC database (http://georoc.mpch-mainz.gwdg.de/georoc/; Sarbas, 2008). Accordingly, high As concentrations in waters adjoin major orogenic belts with past or present volcanic activity (Nordstrom, 2012; Mukherjee et al., 2019). For instance, in Latin America at least 15 countries are affected by high As concentrations in waters and soils from geothermal fields and volcanic systems of the Andean Cordillera (Morales-Simfors et al., 2020). In the Chaco-Pampean plain of Argentina, an area of approximately 1×10^6 km^2 situated to the southeast of the study area (Fig. 1), a vast rural population of 2–8 million inhabitants is exposed to high As concentrations (< 10–5300 μg/L) and other trace elements such as F, V, U, B, Se, Sb, and Mo have affected groundwater quality (Nicolli et al., 2012). Their primary source is the dissolution of rhyolitic volcanic ashes from distal volcanic eruptions in the Andean arc (Smedley et al., 2002; Nicolli et al., 2012; Bia et al., 2022). These ashes were transported by wind and were mixed with calcareous loess-type sediments hosting aquifers. In the arid and semiarid plateaus of north-central Mexico, aquifers adjacent to the Sierra Madre Occidental and Trans-Mexican volcanic belt contain high As (and F) concentrations (Mahlknecht et al., 2004; Morales et al., 2015; Alarcón-Herrera et al., 2020). These elements have an origin in the dissolution of fragments of volcanic rocks such as rhyolitic ignimbrites and glass present in aquifer sediments resulting in an exposure of an estimated 8.81 million people (Alarcón-Herrera et al., 2020). In the Western United States, non-thermal groundwater surrounding the Western Mountain Ranges containing concentrations of As between 10 and 50 μg/L, and in some cases >50 μg/L, are most commonly associated with areas underlain by volcanic rocks of silicic to intermediate composition and their sedimentary byproducts (Welch et al., 1988; Robertson, 1991). In other regions of the world such as central and southern Italy, groundwater hosted in volcanic aquifers and/or discharge from thermal reservoirs exceed the permitted concentrations of As (and other elements such as F and Rn) for human consumption (Aiuppa et al., 2003, 2006; Angelone et al., 2009; Cinti et al., 2015, 2019). In the Porto Santo Island, Portugal, groundwater containing >10 μg/L of As (and other components like F, B, and V) is associated with the leaching of hyaloclastites composed predominantly (90%) of trachytic and rhyolitic volcanic glass (Condesso de Melo et al., 2020). In the rhyolitic volcanic area of Lesvos Island, Greece, As concentrations ranging from 1.8 to 54.7 μg/L were found in groundwater (Zkeri et al., 2015; Zkeri et al., 2018). Silicate weathering and pH-related desorption of As, primarily from Fe mineral phases, were identified as the main processes that enhanced As mobility (Zkeri et al., 2015). In the Main Ethiopian Rift area, the waters often exceed the allowed concentrations of As (and F) for human beings as a consequence of the leaching of rhyolitic volcanic rocks and volcanic glass (Rango et al., 2013; Bianchini et al., 2020).

As highlighted above, most evidence indicates that silicic (mostly rhyolitic) volcanic rocks, and particularly glass-rich ash tend to be responsible for most of the high As concentrations in waters of volcanic regions. It is known that the concentration of As in the bulk Earth (~1.7 mg/kg) is strongly partitioned toward the upper crust (Table 1; Rudnick and Gao, 2005, 2014). The two orders of magnitude difference between the concentration in the mantle and that in the upper crust (Table 1), suggests that As segregated into the crust as the Earth formed and likely continued to accumulate in the upper crust during the Earth's 4.55 billion year evolution. Regarding common rocks, the highest As concentration is found in sulfide mineral deposits especially those containing gold. Next highest are marine shales, followed by rhyolite and non-marine shales, etc. (Table 1). Similar high concentrations for marine shale and rhyolite are found in the evaluated samples compiled by Hu and Gao (2008).

The actual cause of high As concentrations in magmas, and the mobility and partitioning of As among the different type of volcanic products (solid/gas phases) during eruptions is still poorly constrained (López et al., 2012; Morales-Simfors et al., 2020). Arsenic is a volatile element which is considered to partition from the magmatic melt into a magmatic vapor phase during volcanic eruptions, mostly forming OH and S complexes (Simon et al., 2007; Zajacz et al., 2008; Borisova et al., 2010). However, the ability of As to partition out of the melt depends on different aspects that control the presence both of a vapor phase and of ligands, or elements in the exsolving vapor (and/or saline fluid) (Hedenquist and Lowenstern, 1994; Williams-Jones and Heinrich, 2005). If the magma reaches the surface by an eruption, considerable

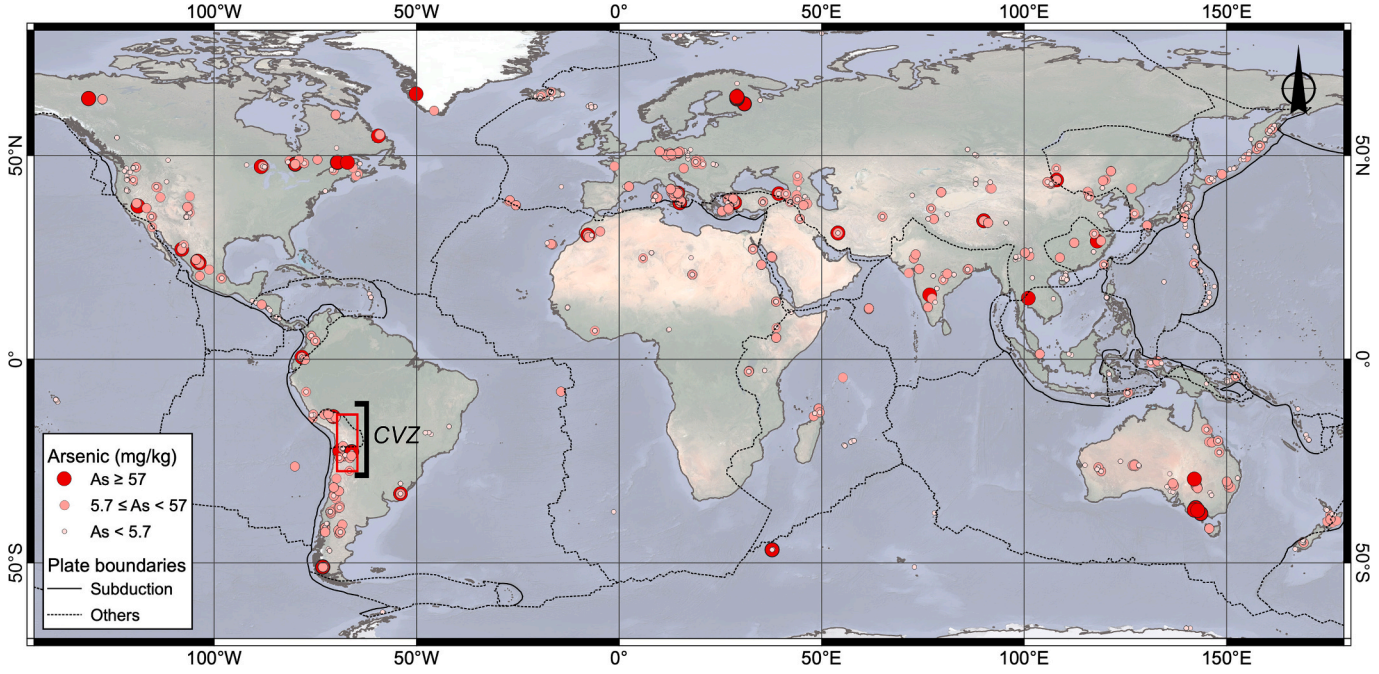

Fig. 1. Global distribution and concentrations of As in all types of volcanic rocks according to GEOROC data base. The Altiplano-Puna region situated in the Central Volcanic Zone (CVZ) of the Andes is marked with a red rectangle. Map made using QGIS, base map obtained from Google Satellite, and plate tectonics from Bird (2003). (For interpretation of the references to colour in this figure legend, the reader is referred to the web version of this article.)

Table 1
Known distribution of As within the Earth and common rocks.

Earth component	As (mg/kg)	Reference
Bulk Earth	1.7	Rudnick and Gao (2005)
Mantle	0.068	Palme and O'Neill (2014)
Lower continental crust	0.2	Rudnick and Gao (2014)
Middle continental crust	3.1	Rudnick and Gao (2014)
Upper continental crust	4.8	Rudnick and Gao (2014)
Seawater	1.7 (μg/L)	(Neff, 2002)
Rock Type[*]		
Gold ore	180 (conservatively low)	USGS and GSJ
Marine shale	68.5	USGS and GSJ
Rhyolite	19	USGS and GSJ
Non-marine shale	6	USGS and GSJ
Limestone	1.6	USGS and GSJ
Sandstone	1	USGS and GSJ
Andesite	0.88	USGS and GSJ
Granite	0.8	USGS and GSJ
Basalt	0.4	USGS and GSJ
Dunite	0.034	USGS and GSJ

[*] Compilation of As concentrations in common rocks from standard rock samples after the US Geological Survey (USGS) and the Geological Survey of Japan (GSJ) (Flanagan, 1976 and Japanese Geochemical Reference samples Database https://gbank.gsj.jp/geostandards).

degassing will take place and As can partition into the vapor phase at high temperature, but it can also sorb onto ash particles. Arsenic has a strong affinity for sulfur so that partitioning is strongly affected by the amount of sulfur in the system as well as temperature and pressure and other compositional variables (Hedenquist and Lowenstern, 1994; Williams-Jones and Heinrich, 2005; Simon et al., 2007; Zajacz et al., 2008; Borisova et al., 2010).

In spite of the importance of volcanic rocks as a geogenic source of As in the planet Earth, variations of As concentration within different types of volcanic rocks are not yet fully understood (Smedley and Kinniburgh, 2002; Bowell et al., 2014). Specifically, in the Altiplano-Puna plateau, the Cenozoic volcanism is considered the source of As for most of the water types in a wide range of concentrations: acid mine drainage (AMD; 25,000 μg/L); brines (16,800 μg/L); rivers affected by AMD (2800 μg/L); hot springs (1900 μg/L); saline waters (1900 μg/L); rivers and lakes (600 μg/L); groundwater (200 μg/L) (Ormachea Muñoz et al., 2013, 2015, 2016; Murray et al., 2019; Tapia et al., 2019). In spite of several publications on volcanology and petrology describing and interpreting this important volcanic system, our current knowledge of As on its volcanic rocks is poor. Therefore, the aim of this work is to contribute a better understanding of the origin and distribution of As in the volcanic rocks of the Altiplano-Puna plateau as a geogenic source of As in water. This work also discusses different factors that may control the origin and the distribution of As in volcanic rocks that could also explain the presence of As in other volcanic regions of the planet such as i) the source and composition of the magmas; ii) the eruptive dynamics; and iii) post-emplacement processes.

2. Settings of the Altiplano-Puna plateau

The Altiplano-Puna plateau in the Central Andes extends through parts of Argentina, Bolivia, Chile, and Peru. This plateau occupies a surface area of 5×10^5 km^2 (Allmendinger, 1986) at an elevation of about 4 km a.s.l. (Lamb and Hoke, 1997; Fig. 1), and extends 1800 km from N to S, with a width of 350–400 km (Allmendinger et al., 1997). The Altiplano-Puna, constitutes a thickened continental crust of up to 70 km (e.g., Yuan et al., 2002) and is the second highest plateau on Earth after Tibet (Allmendinger et al., 1997). The region is composed of two distinctive zones: the Altiplano of Bolivia and Peru, and the Puna of northwestern Argentina and adjoining parts of Chile (Fig. 2).

The Central Volcanic Zone (CVZ) of the Central Andes of South America extends through the Altiplano-Puna plateau and further west (Fig. 1). The CVZ is the segment of the Andean volcanic arc between 14 and 27°S (Stern, 2004) where tens of active volcanoes are found and >15.000 km^3 of ignimbrites (see definition in the Glossary, Supplementary Material) were formed during the Miocene to Recent (e.g., de Silva et al., 2015); thus it is one of the largest ignimbritic provinces of the world (e.g., Francis and Baker, 1978; Best et al., 2016). The CVZ hosts a substantial amount of volcanic rocks in which three main types of volcanic edifices can be recognized: i) stratovolcanoes, ii) collapse calderas and iii) scoria cones associated to monogenetic volcanism (e.g. Kay and Coira, 2009; Grosse and Guzmán, 2017; Wörner et al., 2018). Between 24 and 15 Ma, the characteristic closed drainage system of the Altiplano-Puna was established and the arid climate facilitated the formation of evaporite deposits (Fig. 2) (Alonso et al., 1991; Vandervoort et al., 1995). The closed basins of the plateau were filled with significant volumes of clastic material and chemical weathering products from the surrounding mountain ranges (Igarzábal, 1999), as well as extensive volcanic deposits such as ignimbrites and lavas (e.g., Kay and Coira, 2009). In this region, the altitude (> 3500 m a.s.l.) and width (≈ 400 km) of the Andes produces distinctive meteorological conditions making it one of the highest arid to semi-arid regions on Earth (Gregory-Wodzicki, 2000). Water is a scarce resource in the plateau and it is naturally enriched in As with values above the limit for human consumption. The estimated population is of about 3 million inhabitants who are mainly descendants from aboriginal communities and, in many cases, use untreated water for drinking and cooking purposes (Tapia et al., 2019).

3. Methodology

The data presented in this work comes from a thorough bibliographic compilation extracted from existing publications on petrology and volcanology in the Altiplano-Puna reporting As concentrations in volcanic rocks (Table 2 and Table S1). The access to unpublished As data in some of these publications was made thanks to co-authorship by Silvina Guzmán. The compilation includes As data from different volcanic centers and volcanic outcrops in the Altiplano-Puna of Argentina (15), Bolivia (28), and Chile (12). The data source was self-evaluated for validity and representativeness. In total, 262 As analyses were obtained from 20 publications up to January 2022. We also compiled data for major oxides, trace elements and age of the rocks that contain As concentration data. The presence and type of hydrothermal alteration described were also considered. Samples with non-reported hydrothermal alteration were classified as "non-altered", and those with reported hydrothermal alteration were classified as "with alteration". In these publications, geochemical determinations for As were obtained from bulk samples, the measurements correspond to total As. The analytical methods used for As determinations mainly included inductively coupled plasma mass spectrometry (ICP-MS), inductively coupled plasma atomic emission spectrometry (ICP-AES), induced neutron activation analysis (INAA), and X-Ray Fluorescence (XRF). Most of the publications provide information on analyses quality (e.g., Torres et al., 2021; Ureta et al., 2021) in which data on used Certified Reference Materials and analytical precision are given. In other cases, authors only mention the name of the commercial/university laboratory and the analytical technique used (e.g., Mattioli et al., 2006; Salado Paz et al., 2018). For the statistical analysis, those samples with As values below the detection limit (<0.6 mg/kg) were replaced by half of the detection limit value in order to consider the very low measured As concentrations.

Major oxides were recalculated to a free volatile basis considering the values given for loss on ignition (LOI), CO_2, and SO_3 provided in the different publications for its classification in the Total Alkali-Silica diagram (TAS: $Na_2O + K_2O$ (wt. %) vs SiO_2 (wt. %); Le Le Maitre, 1989). This is a chemical and non-genetic classification recommended by the IUGS (International Union of Geological Sciences) Subcommission on

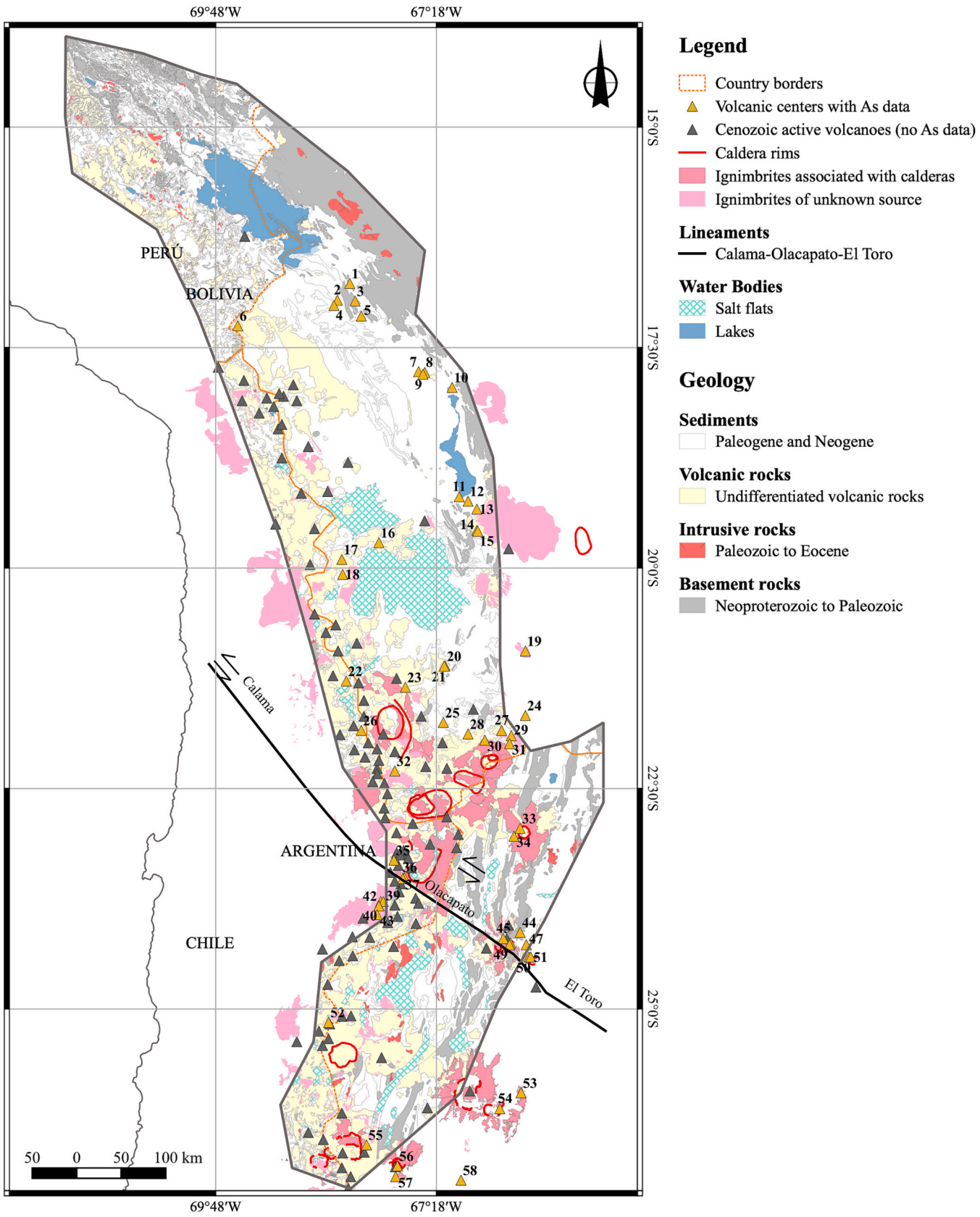

Fig. 2. Geological map of the Altiplano-Puna showing the distribution of Cenozoic volcanic rocks. The numbering of the volcanoes refers to those listed in Table 2.

Table 2
Mean, maximum (max), minimum (min), standard deviation (σ), and median values of As (mg/kg) in volcanic centers and volcanic outcrops in the Altiplano-Puna region. The volcanic center No. corresponds with Fig. 2.

No.	Volcano name	Lat.	Lon.	Volcano type	n	mean	max	min	σ	median	Location	Epoch or period
1	Viacha[a]	−16.770	−68.280	Volcanic outcrop	2	0.8	0.8	0.8	0	0.8	Altiplano, BO	Cenozoic
2	Comanche[a]	−16.960	−68.420	Volcanic outcrop	1	<0.60	–	–	–	–	Altiplano, BO	Middle Miocene
3	Colquencha[a]	−16.970	−68.220	Volcanic outcrop	1	<0.6	–	–	–	–	Altiplano, BO	Cenozoic
4	Miriquiri[a]	−17.020	−68.460	Volcanic outcrop	1	1.3	–	–	–	–	Altiplano, BO	Middle Miocene
5	Viscachani[a]	−17.140	−68.150	Volcanic outcrop	1	1.1	–	–	–	–	Altiplano, BO	Cenozoic
6	La Española[a]	−17.250	−69.550	Volcanic outcrop	4	0.4	0.85	<0.5	0.3	0.3	Cordillera Oriental	Late Miocene
7	La Joya[a]	−17.770	−67.500	Volcanic outcrop	2	56.1	110	2.2	76.2	56.1	Altiplano, BO	Middle Miocene
8	Escatanque[a]	−17.780	−67.430	Volcanic outcrop	1	<0.60	–	–	–	–	Altiplano, BO	Cenozoic
9	Kori Kollo (La Joya district) [a]	−17.800	−67.450	Volcanic outcrop	3	34	74	11	34.8	17	Altiplano, BO	Middle Miocene
10	San José (Oruro)[a]	−17.950	−67.120	Volcanic outcrop	1	110	–	–	–	–	Altiplano, BO	Middle Miocene
11	Stratovolcano deposits (Pampa Aullagas)[b]	−19.190	−67.040	Stratovolcano	2	4.7	4.7	4.6	0.1	4.7	Altiplano, BO	Miocene to Holocene
12	Stratovolcano deposits (Quillacas)[b]	−19.240	−66.940	Stratovolcano	2	1.5	2.6	<0.5	1.6	1.5	Altiplano, BO	Miocene to Holocene
13	Co. Gordo[a]	−19.330	−66.840	Volcanic outcrop	1	<0.60	–	–	–	–	Altiplano, BO	Cenozoic
14	Río Mulato[a]	−19.570	−66.840	Volcanic outcrop	1	<0.60	–	–	–	–	Altiplano, BO	Cenozoic
15	Ignimbrite Los Frailes and Morococala[b]	−19.580	−66.830	Caldera	3	0.9	1.2	0.5	0.4	0.9	Altiplano BO	Miocene
16	Iñexa[a]	−19.710	−67.950	Volcanic outcrop	3	1.1	1.4	0.8	0.3	1.1	Altiplano, BO	Pliocene
17	Chinchilhuma[a]	−19.900	−68.370	Volcanic outcrop	1	0.8	–	–	–	–	Altiplano, BO	Cenozoic
18	Paco Kkollu[a]	−20.070	−68.360	Volcanic outcrop	3	2.2	4.6	1	2.1	1.1	Cordillera Oriental	Late Miocene
19	Chocaya[a]	−20.940	−66.290	Volcanic outcrop	1	1.1	–	–	–	–	Altiplano, BO	Cenozoic
20	Inca Mine[a]	−21.110	−67.200	Volcanic outcrop	2	5.4	6.7	4.1	1.8	5.4	Altiplano, BO	Cenozoic
21	Toldos Mine[a]	−21.110	−67.210	Volcanic outcrop	1	6.5	–	–	–	–	Altiplano, BO	Upper Miocene
22	Ollague-Mafic center[c]	−21.280	−68.320	Shield-like monogenetic	1	5.7	–	–	–	–	Altiplano, CH-BO	Quaternary
23	Sora Puncu[a]	−21.350	−67.650	Volcanic outcrop	1	15	–	–	–	–	Altiplano, BO	Cenozoic
24	Esmoraca[a]	−21.670	−66.290	Volcanic outcrop	1	1.5	–	–	–	–	Altiplano, BO	Miocene
25	Com. Todos Santos[a]	−21.750	−67.220	Volcanic outcrop	2	2.1	2.7	1.5	0.8	2.1	Altiplano, BO	Cenozoic
26	Apacheta-Aguilucho volcanic complex[c]	−21.840	−68.150	Stratovolcano and domes	16	5.4	14	0.8	4.6	5.5	Altiplano CH	Pleistocene
27	Morokho[a]	−21.840	−66.560	Volcanic outcrop	1	2.4	–	–	–	–	Altiplano, BO	Cenozoic
28	S.A. de Lipez[a]	−21.880	−66.940	Volcanic outcrop	1	3.8	–	–	–	–	Altiplano, BO	Cenozoic
29	Loma Grande[a]	−21.900	−66.450	Volcanic outcrop	4	2.2	4.4	1.1	1.5	1.7	Altiplano, BO	Cenozoic
30	Jaquegua[a]	−21.950	−66.750	Volcanic outcrop	2	14.7	23	6.3	11.8	14.7	Altiplano, BO	Cenozoic
31	Panizos Caldera[a]	−21.990	−66.470	Caldera	7	1.5	2.6	<0.6	0.7	1.4	Altiplano, BO	Miocene
32	Co. Pabellón[a]	−22.300	−67.770	Stratovolcano	1	3.8	–	–	–	–	Altiplano, BO	Middle Miocene
33	Coranzulí[d]	−22.950	−66.350	Caldera	13	15.3	126	2.2	33.4	5.5	Northern Puna, ARG	Upper Miocene
34	Morro Grande[d]	−23.040	−66.420	Caldera	18	34.6	325	4	73.5	17.5	Northern Puna, ARG	Miocene
35	Lascar[e]	−23.310	−67.780	Stratovolcano	1	6	–	–	–	–	Central Puna, CH	Holocene
36	Cerro Overo[f]	−23.510	−67.660	Monogenetic center	2	5.1	5.5	4.6	0.6	5.1	Central Puna, CH	Pleistocene
37	La Albondiga[f]	−23.520	−67.680	Monogenetic center	2	5.3	5.6	4.9	0.5	5.3	Central Puna, CH	Cenozoic
38	El País lava flow field[g]	−23.780	−67.930	Monogenetic lava flow	17	2.8	6	2	1.3	2	Central Puna, CH	Plio-Pleistocene
39	Corral Negro [g]	−23.780	−67.900	Stratovolcano	1	6	–	–	–	–	Central Puna, CH	Plio-Pleistocene
40	Cerro Tujle[h]	−23.830	−67.950	Monogenetic center	4	3.6	5.5	1.6	1.8	3.6	Central Puna, CH	Quaternary
41	Lithic xenolite in Cerro Tujle[h]	−23.830	−67.950	Monogenetic center	3	11.4	15	8.2	3.4	11	Central Puna, CH	Cenozoic
42	Tucúcaro ignimbrite[h]	−23.830	−67.950	Ignimbrite field	2	5.5	7.4	3.5	2.8	5.5	Central Puna, CH	Pliocene
43	Cerro Toloncha[h]	−23.930	−67.970	Poligenetic cone	3	2.1	3.6	1	1.4	1.6	Central Puna, CH	Pleistocene
44	Ramadas[i]	−24.130	−66.350	Monogenetic center	1	6	–	–	–	–	COT area, ARG	Late Miocene
45	Tocomar[j]	−24.200	−66.540	Monogenetic center	2	94.7	104	85.3	13.2	94.7	COT area, ARG	Pleistocene

(*continued on next page*)

Table 2 (*continued*)

No.	Volcano name	Lat.	Lon.	Volcano type	n	mean	max	min	σ	median	Location	Epoch or period
46	Cerro San Gerónimo[k]	−24.250	−66.460	Scoria cone	2	9.2	15.8	2.5	9.4	9.2	COT area, ARG	Quaternary
47	El Morro[j]	−24.270	−66.280	Stratovolcano or dome	6	2.5	5.11	1.4	1.4	2.3	COT area, ARG	Miocene
48	Aguas calientes (non-altered ignimbrites)[j]	−24.270	−66.470	Caldera	10	12.5	22.3	3.3	6.2	12.7	COT area, ARG	Miocene
49	Aguas calientes (ignimbrites with alteration)[l]	−24.270	−66.470	Caldera	14	1638	7147	1.7	2270	518	COT area, ARG	Miocene
50	Nuegra Muerta volcanic complex[j]	−24.410	−66.250	Caldera	1	3.4	–	–	–	–	COT area, ARG	Miocene
51	Plutonic-Volcanic center Nevado del Acay[j]	−24.410	−66.230	Plutonic-Volcanic center	3	1.8	3.1	0.8	1.2	1.4	COT area, ARG	Miocene
52	Lastarria[e]	−25.150	−68.520	Stratovolcano	3	20	29	13	8.2	18	Southern Puna, CH	Holocene
53	Alto de Las Lagunas Ignimbrite[m]	−25.950	−66.340	Caldera	2	1.6	1.6	1.6	0	1.6	Southern Puna, ARG	Middle Miocene
54	Luingo[n]	−26.130	−66.580	Caldera	14	1.8	10.9	<0.5	2.9	0.7	Southern Puna, ARG	Middle Miocene
55	Peinado[o]	−26.540	−68.090	Stratovolcano	25	7.4	69.6	<0.5	15.9	1.9	Southern Puna, ARG	Pleistocene
56	Cerro Blanco volcanic complex[p]	−26.780	−67.740	Caldera	5	1	3.3	<0.5	1.3	0.3	Southern Puna, ARG	Quaternary
57	San Buenaventura Cordillera[p, q, r, s, t]	−26.900	−67.760	Caldera	20	1.7	7.2	<0.5	1.9	0.9	Southern Puna, ARG	Upper Miocene
58	Vicuña Pampa[u, v]	−26.940	−67.020	Stratovolcano	14	1	2.7	<0.5	0.8	0.7	Southern Puna, ARG	Miocene
	Volcanic rocks (without hydrothermal alteration)*				238	9.1	325	<0.5	27	2.6	Altiplano-Puna	Cenozoic
	Volcanic rocks (with hydrothermal alteration and sulfide mineralization)*				24	957	7147	0.9	1895	54	Altiplano-Puna	Cenozoic
	Volcanic rocks (all samples)*				262	96	7147	<0.5	626	2.6	Altiplano-Puna	Cenozoic
	Fluvial sediments[w]				1053	107	12,300	1	750	20	Altiplano-Puna	

BO = Bolivia; CH = Chile; ARG = Argentina; COT = Calama-Olacapato-El Toro regional structural lineament.

[a] USGS and SGBO (1975).
[b] Ormachea Muñoz et al. (2013).
[c] Taussi et al. (2019).
[d] Gorustovich et al. (1989).
[e] Robidoux et al. (2020).
[f] Ureta et al. (2021).
[g] Torres et al. (2021).
[h] Ureta et al. (2020a).
[i] Lucci et al. (2018).
[j] Petrinovic et al. (1999).
[k] Mattioli et al. (2006).
[l] Salado Paz et al. (2018).
[m] Aramayo et al. (2017).
[n] Guzmán et al. (2011).
[o] Grosse et al., 2022.
[p] Montero-López (2009).
[q] Montero-López et al. (2010).
[r] Montero-Lápez et al. (2010).
[s] Montero-López et al. (2011).
[t] Montero-López et al. (2015).
[u] Guzmán et al. (2017a).
[v] Guzmán et al. (2017b).
[*] This study.
[w] Tapia et al. (2019).

the Systematics of Igneous Rocks for the classification of volcanic rocks (Le Bas and Streckeisen, 1991). The Aluminum Saturation Index (ASI) was also used. This index is based on molecular Al/(Ca – 1.67P + Na + K) (Rollinson and Pease, 2021 and references therein) and it defines rocks as peraluminous (ASI > 1) or metaluminous (ASI < 1). Metaluminous rocks lack the necessary Al needed to form feldspars and peraluminous rocks are rich in Al, with more than what is needed to form feldspars. Peraluminous rocks are generally derived from the melting of clay-rich sedimentary sources (Rollinson and Pease, 2021 and references therein).

The data for the world map showing the As concentration in volcanic rocks (Fig. 1), was extracted from GEOROC database (http://georoc.mpch-mainz.gwdg.de/georoc/; Sarbas, 2008). The free and open source Quantum Geographic Information System (QGIS) was used for the maps edition and calculation of the surface covered by volcanic rocks in the Altiplano-Puna using the polygon area function. A Glossary (see Supplementary data) was made to describe terms related to volcanology and petrology taken mostly from Sigurdsson et al. (2015).

4. Results

4.1. Mean As concentrations in volcanic rocks of the Altiplano-Puna

The mean As concentration in volcanic rocks of the Altiplano-Puna, considering samples without reported hydrothermal alteration (n = 238), is 9.1 mg/kg with a median of 2.5 mg/kg and maximum value of 325 mg/kg (Table 2). Volcanic rocks with hydrothermal alteration and sulfide mineralization (n = 24) have a mean value of 957 mg/kg with a median of 54 mg/kg and maximum of 7147 mg/kg (Table 2). Considering both type of samples (n = 262), the total average of As in volcanic rocks is 96 mg/kg (Table 2).

The following sections describe the variations of As concentrations according to the geochemical composition of the rocks, presence or lack of hydrothermal alteration, sulfide mineralization, type of volcanic edifice, type of volcanic deposits, and spatial distribution.

4.2. Arsenic concentrations according to the geochemical composition and hydrothermal alteration of volcanic rocks

Most of the volcanic rocks of the Altiplano-Puna plateau show a SiO_2 content from intermediate (52–63% wt. SiO_2) to silica-rich (> 63% wt. SiO_2) compositions. When comparing the As concentration variation with SiO_2, it is observed that the highest As values are present in silica-rich samples, particularly in those rocks with hydrothermal alteration (Fig. 3).

In the Altiplano-Puna plateau, rocks with As reported data show a wide range of compositional types from basaltic andesites to rhyolites (Table 3; Fig. 4). In the TAS diagram (Fig. 4), it is observed that the As concentrations tend to increase with the amount of alkalis ($Na_2O + K_2O$) and SiO_2 content. In non-altered volcanic rocks, mean values of As increases progressively with increasing silica, from basaltic andesites (3.2 mg/kg) to andesites (3.5 mg/kg), and from dacites (11.3 mg/kg) to rhyolites (19.8 mg/kg) (Fig. 4 a; Table 3). When rocks have hydrothermal alteration and/or sulfide mineralization they are mainly silica-rich and the concentration of As increases, especially for trachydacites (181 mg/kg) and rhyolites (1863 mg/kg) (Fig. 4 b; Table 3).

Regarding Aluminum Saturation Index (ASI) and As concentrations, it is observed that peraluminous volcanic rocks (i.e. those that have a clay-rich or shale type of sedimentary source) have higher As concentrations (average of 203 mg/kg; Table 4) than metaluminous varieties (average of 4.7 mg/kg; Table 4). In addition, peraluminous rocks with high As concentrations are also silica-rich (Fig. 5).

Table 3
Arsenic concentrations (mg/kg) in volcanic rocks of the Altiplano-Puna with different types of geochemical compositions according to the TAS classification diagram. Mean, maximum (max), minimum (min), standard deviation (σ), and median values.

TAS classification	n	mean	max	min	σ	median
Non-altered						
Basaltic-andesite	24	3.2	6.0	1.4	1.6	2.0
Basaltic-trachyandesite	14	1.8	6.7	0.3	1.9	0.9
Andesite	22	3.5	10.0	0.3	2.7	3.7
Trachy-andesite	25	5.3	29.0	0.3	8.0	1.5
Dacite	71	11.3	126.0	0.3	23.5	2.7
Trachy-dacite	33	4.5	20.0	0.3	5.3	1.9
Trachyte	2	5.3	6.5	4.1	1.7	5.3
Rhyolite	37	19.8	325.0	0.3	56.7	3.5
With hydrothermal alteration						
Trachy-andesite	2	0.4	0.6	0.3	0.2	0.4
Dacite	5	10.5	31.4	0.3	13.9	1.7
Trachy-dacite	3	181	541	0.3	312	2
Trachyte	1	6.7	–	–	–	–
Rhyolite	12	1863	7147	1	2386	693

TAS = Total Alkali-Silica.

4.3. Arsenic concentrations in different types of volcanic edifices and deposits

4.3.1. Types of volcanoes

In the Altiplano-Puna plateau, the three main different types of volcanoes (monogenetic volcanoes, stratovolcanoes, and collapse calderas) show increasing average As concentrations (Table 5; Fig. 6).

Monogenetic volcanoes (which typically form scoria cones, lava flows and/or domes) are usually characterized by their effusive character or low explosivity. They are mainly of basaltic andesite to andesitic compositions and are associated with deep faults that allow a rapid magma ascent from the mantle (Ureta et al., 2020b). They contain mean As concentrations of 5.2 mg/kg (Table 5). Some monogenetic volcanoes of silicic composition such as Ramadas (rhyolitic pumice that recorded crustal contamination; Coira et al., 2018; Lucci et al., 2018; Bardelli et al., 2021) and Tocomar (ignimbrites or crustal origin; Petrinovic et al.,

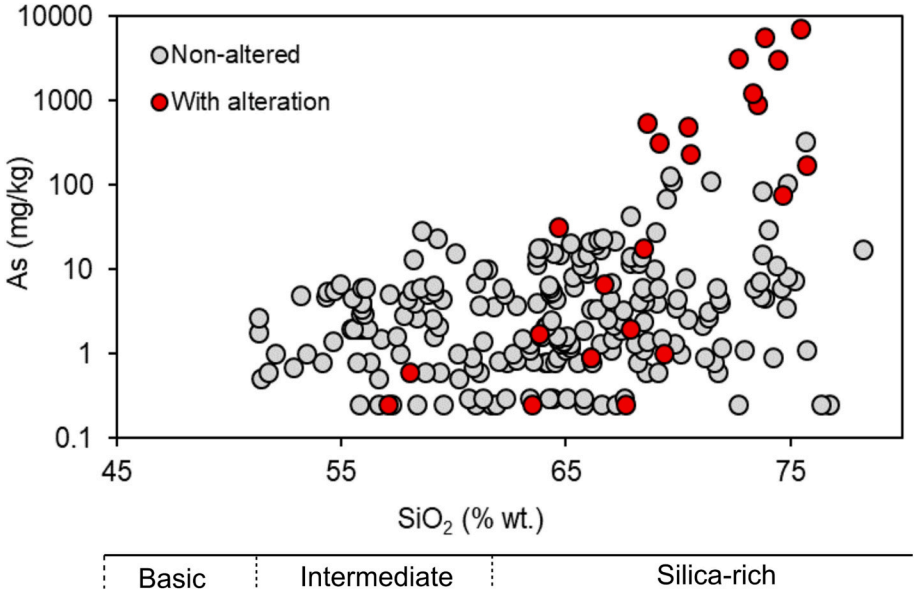

Fig. 3. As (mg/kg) vs. SiO_2 (wt. %) in volcanic rocks of the Altiplano-Puna plateau.

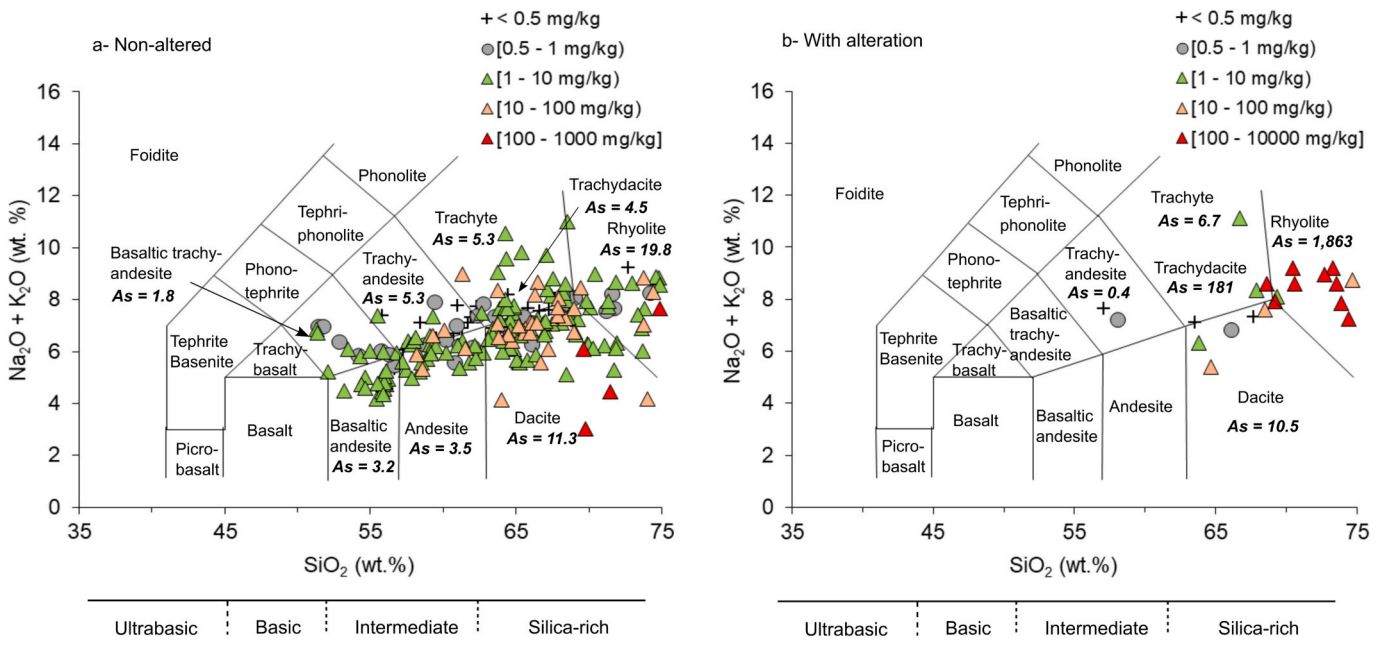

Fig. 4. Total Alkali-Silica diagram (TAS) for volcanic rocks in the Altiplano-Puna plateau. For each compositional field, the As mean value (bold italic) is indicated in mg/kg. a)- Non altered volcanic rocks. b)- Volcanic rocks with reported hydrothermal alteration and/or sulfide mineralization.

Table 4
Mean, maximum (max), minimum (min), standard deviation (σ), and median values of As (mg/kg) in metaluminous and peraluminous volcanic rocks of the Altiplano-Puna.

ASI classification	n	mean	max	min	σ	median
Metaluminous volcanic rocks	130	4.7	69.6	0. 3	8.7	1.7
Peraluminous volcanic rocks	120	203	7147	0.3	916	4.6

ASI = Aluminum Saturation Index (ASI = Al/(Ca – 1.67P + Na + K); Rollinson and Pease, 2021 and references therein).

2006), show higher As content such as 6 mg/kg and 94.7 mg/kg, respectively (No. 44–45, Table 2).

Stratovolcanoes, which are characterized by moderate to high explosivity usually have andesitic to dacitic compositions with mean As concentrations of 5.8 mg/kg (Table 5).

For collapse calderas, which are characterized by highly explosive eruptions with dacitic to rhyolitic compositions, the mean As concentrations increases up to 7.3 mg/kg (Table 5). Some extremely high values are observed in Aguas Calientes caldera in which hydrothermally altered ignimbrites (with sulfide mineralization) present mean As concentrations of 1638 mg/kg (Salado Paz et al., 2018; No. 49, Table 2). In this caldera, the Incachule geothermal springs have an As content of 258 μg/L (Sanci et al., 2020). Other undifferentiated volcanic outcrops

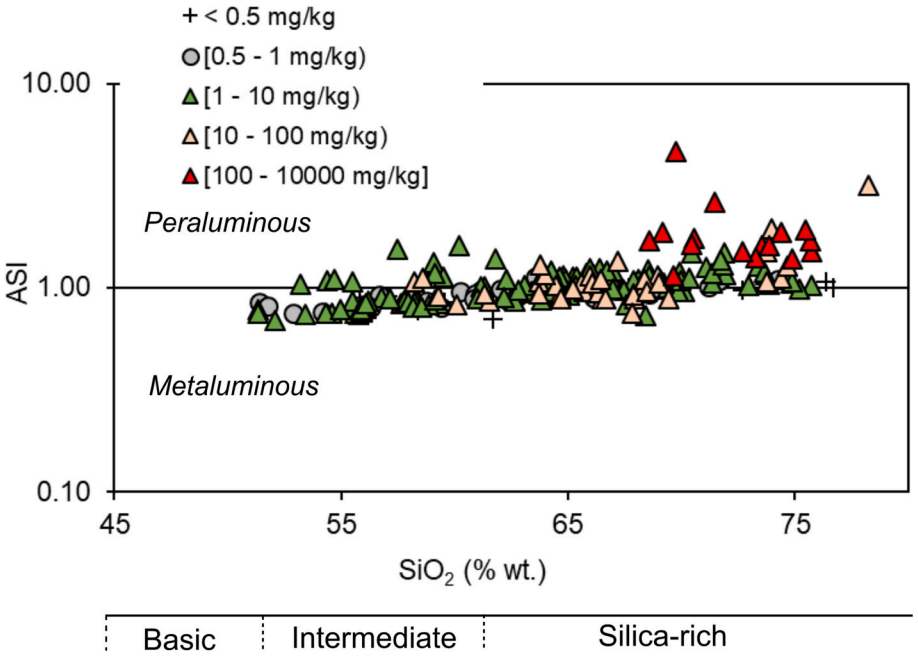

Fig. 5. Aluminum Saturation Index (ASI) vs SiO_2 content and As concentrations in volcanic rocks of the Altiplano-Puna plateau. ASI = Al/(Ca – 1.67P + Na + K).

Table 5
Mean, maximun (max), minimun (min), standar deviation (σ), and median As concentrations (mg/kg) in the three main different types of volcanic edifices of the Altiplano-Puna. *n* = number of volcanoes with As data.

Type of volcano	n	mean	max	min	σ	median
Monogenetic centers, lava flows, scoria cones[1]	9	5.2	11.4	1.8	3.2	5.1
Stratovolcanoes and domes	10	5.8	20	1	5.4	5.1
Calderas and ignimbrite fields[2]	12	7.3	34.6	0.9	10.3	1.8
Undifferentiated volcanic outcrops in the Bolivian Altiplano	25	13.1	110	0.4	26.7	2.2

[1] Ramadas and Tocomar monogenetic volcanoes were not considered since they are silicic in composition and record crustal contamination or origin, the As content for these volcanoes can be seen in Table 1.

[2] The strongly altered and sulfide mineralized ignimbrites from Aguas Calientes caldera (Salado Paz et al., 2018) were not considered; the As content for these rocks can be found in Table 1.

situated in the Bolivian Altiplano have mean As concentrations of 13.1 mg/kg (Table 5).

4.3.2. Volcanic deposits

Arsenic data for the following different type of volcanic deposits, *syn*-volcanic intrusions and structures are available in the literature of the Altiplano-Puna: fall deposits (ash and pumice), deposits of pyroclastic density currents (including ash-flow tuff, block and ash flow, ignimbrite, and tuff) and coherent deposits (domes, dikes, and lavas) (Table 6). A detailed definition of each type of deposit and their characteristics are provided in the Glossary (Supplementary material).

The highest As concentrations are found among deposits of pyroclastic density currents and fall deposits. The Morro Grande tuff (in Northern Puna) contains 325 mg/kg of As (No. 34, Table 1; Gorustovich et al., 1989). Ashes from Peinado stratovolcano contain 43.2 mg/kg of As (Grosse et al., 2022). Ignimbrites without hydrothermal alteration, contain mean values of 11.2 mg/kg of As (Table 5). Altered ignimbrites have the highest As concentrations, however this is mainly related to the post-emplacement enrichment processes rather than the eruptive process (Section 5.1). Pumice, which is mainly composed of silicic glass, has mean values of 14.5 mg/kg of As. Finally, extrusive deposits like lavas (3.7 mg/kg) and those related to domes (6.2 mg/kg), and shallow *syn*-volcanic intrusive bodies as dikes (1.5 mg/kg) that may feed extrusive deposits show generally lower As concentrations.

4.4. Spatial variation of As concentrations

Volcanic edifices and deposits, thermal springs, and sulfide deposits situated along the regional Calama-Olacapato-El Toro (COT) lineament show very high As concentrations (area with outcropping volcanoes from No. 44 to 51, Table 2, Fig. 2). Several authors indicate that magmatism and hydrothermal fluid circulation is strongly controlled by the

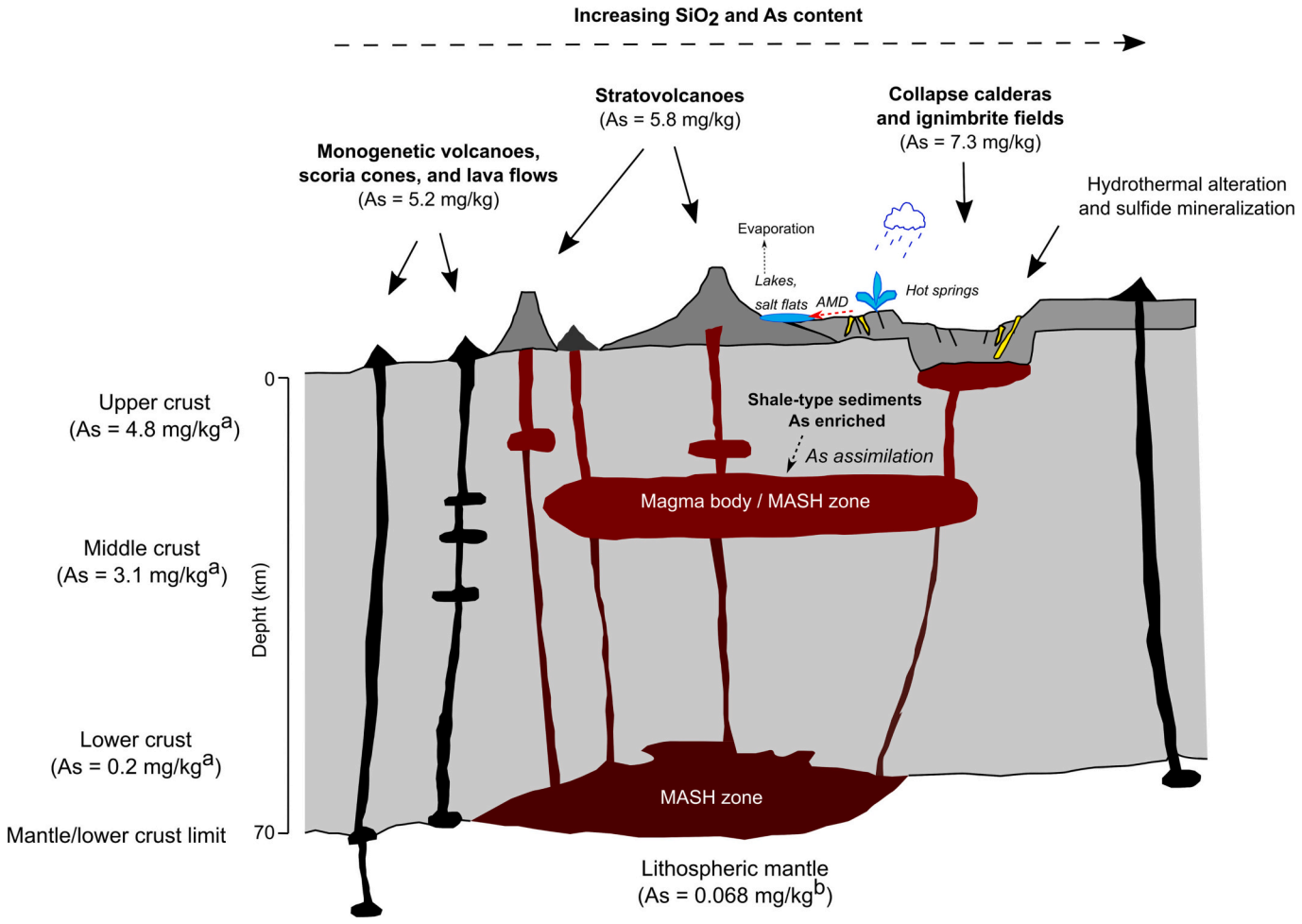

Fig. 6. Schematic model showing As concentrations variations in the three main different types of volcanoes in the Altiplano-Puna plateau and water-rock interactions favoring As enrichment in waters. The assimilation of As enriched shale-like sediments into the magmas is considered as the main As source for magmas in the Altiplano-Puna. Arsenic concentrations values for the crust and the lithospheric mantle belong to the international literature: *a* = Rudnick and Gao (2014) and *b* = Palme and O'Neill (2014). Figure adapted after de Silva and Kay (2018), Wörner et al. (2018), and Murcia and Németh (2020).

Table 6
Mean, maximum (max), minimum (min), standard deviation (σ), and median values for As (mg/kg) concentrations in different types of volcanic deposits in the Altiplano-Puna region.

Type of deposit/structure		n	mean	max	min	σ	median
Fall deposits	Ash	1	43.2				
Pyroclastic	Pumice	5	14.5	69.6	0.3	25.7	1.3
Non-pyroclastic deposits and structures	Dome	8	6.2	14	1.0	5.8	4.3
	Dike	11	1.5	6.0	0.3	1.7	0.9
	Lava	84	3.7	29	0.3	5.2	2.0
Pyroclastic density currents	Ash-flow tuff	18	3.8	23	0.3	5.8	1.5
	Block and ash flow	5	0.7	1.9	0.3	0.7	0.3
	Ignimbrite (non-altered)	75	11.2	126	0.3	21.4	4.5
	Ignimbrite (altered)	19	1638	7147	1.7	2270	518
	Tuff	1	325				

COT structure (Petrinovic et al., 2006; Ramellow et al., 2006; Acocella et al., 2011; Giordano et al., 2013; Lanza et al., 2013; Norini et al., 2013; Filipovich et al., 2022). Along this regional lineament, the Aguas Calientes caldera (No. 49, Table 2; Fig. 2) show the highest As values compiled in this study (mean of 1638 mg/kg) corresponding to altered and sulfide mineralized ignimbrites. The non-altered Aguas Calientes caldera ignimbrites also present high values (mean of 12.5 mg/kg) (No. 48; Table 2). Associated with this caldera, the Incachule hot springs have As concentrations of 258 μg/L (Sanci et al., 2020). Monogenetic centers such as Tocomar (mean of 94.7 mg/kg) (No. 45; Table 2), Cerro San Gerónimo (mean of 9.2 mg/kg) (No. 46; Table 2) and Ramadas (mean of 6 mg/kg) (No. 44; Table 2) contain As concentrations which are above the mean values for this type of volcanic edifices, being Tocomar and Ramadas silica-rich volcanic centers. Hot springs in this area like Pompeya have As concentrations up to 8490 μg/L (Hudson-Edwards and Archer, 2012; Sanci et al., 2020), while Baños de Aguas Calientes hot springs have As concentration of about 2200 μg/L (Hudson-Edwards and Archer, 2012). In addition, in this area, mining wastes from two legacy mining activities (Mina Concordia and La Poma treatment plant) of Pb-Ag-Zn sulfide minerals release Acid Mine Drainage (AMD) with As concentrations between 267 and 8700 μg/L (Kirschbaum et al., 2012; Sanci et al., 2020). This sulfide mineralization is associated with epithermal deposits emplaced into Miocene dacitic domes. Arsenic is mainly present in As-rich pyrite and arsenopyrite that are abundant in the mining wastes (tailings and dumps) (Kirschbaum et al., 2012). The oxidation of these minerals releases As which is then solubilized into waters at low pH (AMD) reaching the rivers and streams in the area. This source of As is originally associated with the Cenozoic volcanism and is further enhanced by human activities.

To the north of the COT structure, in the Northern Puna (Alonso et al., 1984), the Coranzulí and Morro Grande ignimbrites related to caldera systems (Guzmán et al., 2020) also have high As concentrations with mean values of 15.3 mg/kg and 34.6 mg/kg respectively (No. 33–34, Table 2, Fig. 2, Gorustovich et al., 1989). In this area, there is also an active geothermal system with As concentrations between 4.8 and 90 μg/L and temperatures around 20 °C (Peralta Arnold et al., 2017). Legacy mining activities associated to Miocene dacitic domes are also present in Northern Puna (Mina Pan de Azúcar). The source of As is also related to the oxidation of pyrite and arsenopyrite in tailings dams and dumps, and the As concentrations released into waters can be as high as 44,600 μg/L (Murray et al., 2014, 2021).

Northwards, the concentrations of As in the Altiplano of Bolivia and Chile vary from 1.1 to 110 mg/kg (No. 1–32, Table 2, Fig. 2), with the highest values associated with polymetallic deposits (i.e., La Joya, Kiri Kollo, and San José).

In contrast, the volcanic centers situated in the Southern Puna (No. 52–58, Table 2, Fig. 2) show lower As contents such as the ignimbrites of Cerro Blanco volcanic complex and San Buenaventura Cordillera with mean As concentrations of 1 mg/kg and 1.7 mg/kg, respectively. For instance, Vicuña Pampa volcanic complex have mean As contents of 1 mg/kg, and Alto de Las Lagunas ignimbrites show a mean value of 1.6 mg/kg. In Luingo caldera, the mean values are of 1.8 mg/kg. In the case of the Peinado stratovolcano situated in the western part of the Southern Puna, it shows a higher mean value of 7.4 mg/kg which is mostly related to high As concentration in glass-rich components as ashes and pumices (43.2–69.6 mg/kg), while the As concentration in lavas varies between <0.5 mg/kg and 4.7 mg/kg.

5. Discussion

5.1. Factors controlling As concentrations in volcanic rocks

Based on the compiled data, three main factors were found that can explain the relatively high As concentrations in volcanic rocks: i) the source and composition of the magmas (related to the area in which magmas were first generated, the possible assimilation of As-enriched crustal rocks, and the final composition of the evolved volcanic products); ii) the eruptive dynamics, particularly in those deposits related to explosive eruptions; iii) the post-emplacement enrichment processes of volcanic deposits by hydrothermal alteration and/or exsolution of volatiles from the active magmatic reservoir. Each factor is explained in detailed below.

i) The source and composition of the magmas: it is known that As concentration in the mantle, where some magmas are originated, is low (0.068 mg/kg; Palme and O'Neill, 2014 Table 1). This value increases from the lower to the middle continental crust (0.2 to 3.1 mg/kg), while the upper continental crust is highly enriched in As with a value of 4.8 mg/kg (Fig. 6; Table 2 Rudnick and Gao, 2014). In the Altiplano-Puna plateau, at upper crustal levels two large magma bodies are interpreted as feeding magma chambers of volcanoes. These main bodies are known as the Altiplano-Puna Magma Body (APMB, Zandt et al., 2003) and the Southern Puna Magma Body (SPMB, Bianchi et al., 2013). The APMB is situated between the Northern Puna and the Bolivian Altiplano and is one of the largest active continental crustal magma body on Earth (Perkins et al., 2016). The SPMB is of smaller dimensions and is situated in the Southern Puna. In these magma bodies MASH (melting-assimilation-storage-homogenization of the crust; Hildreth and Moorbath, 1988; Fig. 6) processes occurs (e.g. de Silva and Kay, 2018 and references therein). Moreover, these melted magma bodies receive inputs of mantle-derived magmas that underlie the volcanic region (e.g. de Silva and Kay, 2018 and references therein).

The chemical compositions of the ignimbrites situated above the APMB and geochemical modeling of trace elements and radiogenic isotopes show a roughly equal contribution from crustal and upper mantle sources (e.g. Kay et al., 2010; Perkins et al., 2016). As described in Section 4.4, the volcanic outcrops situated in the Northern Puna of Argentina present higher As concentrations than those situated in the Southern Puna maybe indicating the effect of As assimilation from the originally As-enriched continental crust. In the northern and central region of the Puna, the basement has a strong component of shales-type deposits with very low metamorphic grade (i.e., the Acoite Formation) that contains high As concentrations (7–124 mg/kg; Bierlein et al., 2006) and a strong gold mineralization with high As content (Rodríguez et al., 2001; Rodríguez and Bierlein, 2002). Remarkably, Kay et al. (2010) indicated that in the most peraluminous ignimbrites of the Granada–Orosmayo–Cusi Cusi, Vilama, Panizos, and Coranzulí magmas, the highest isotopic $^{87}Sr/^{86}Sr$ ratios (0.712–0.720) fit with a shale-type component. From these set of rocks, available As data are those from Coranzulí ignimbrites which contain an average of 15.3 mg/kg of As (No. 33, Table 2). Toward the Chilean Altiplano, the andesitic magmas of the Apacheta-Aguilucho stratovolcanoes and nearby domes (with 5.4

mg/kg of As) (No. 26, Table 2) were affected by a process of assimilation and fractional crystallization during their ascent through the upper crust, which is composed of Eocene-Miocene basement (sequence of andesitic lava flows, conglomerates, breccias, sandstones, limestones, and gypsum formations) (Taussi et al., 2019). Also, the magmas that originated the high-K andesitic lavas outcropping in the vicinity of the Ollagüe mafic center (with 5.7 mg/kg of As) (No. 22,Table 2) are mantle derived and were contaminated with the Paleozoic basement (gneiss and metabasites) during a rapid uprising through the thick crust, without any storage and differentiation in magma chambers (Mattioli et al., 2006). Crustal assimilation as a source of As in magmatic arcs was hypothesized by Mukherjee et al. (2019). By assessing the case studies in which evolution patterns of magmas are known from the literature, and where the type of assimilated material has been identified, we suggest a strong correlation between assimilation of shale-type sediments and high As concentrations in volcanic rocks. Furthermore, this important process of crustal assimilation is enhanced in the Altiplano-Puna plateau and Central Volcanic Zone of the Andes where the crust is extremely thick (up to >70 km) favoring the development of large magma bodies where MASH process take place (Fig. 6).

A contrasting example to As-enriched magmas is provided by the As-depleted monogenetic volcanoes whose magmas are connected to mantellic-lower crust sources (Fig. 6) and experienced rapid ascents with low crustal contamination such as El País lava flow field (Torres et al., 2021). The mean As content of this monogenetic unit is of 2.8 mg/kg (No. 38, Table 2).

In the case of volcanic rocks situated along the COT lineament, which is an important tectonic transfer zone for magmas and circulation of geothermal fluids (Section 4.4), the rhyolites of the Ramadas monogenetic center (6 mg/kg of As) (No. 44, Table 2) have an origin in a silicic crystal-mush reservoir which show mixtures of mantle-derived magmas with crustal melts containing meta-pelitic components (Coira et al., 2018; Bardelli et al., 2021). Also, the Tocomar rhyolitic ignimbrites, with very high As concentrations (94.7 mg/kg of As) (No. 45, Table 2), show a significant contribution of crustal shale-type components in the magma (Petrinovic et al., 2006). The presence of regional structures, the circulation of geothermal fluids, and the thickened crust have been proposed as main factors controlling high As concentrations in the Puna-Altiplano of Chile (Tapia et al., 2021; Tapia et al., 2022).

Toward the Southern Puna, As concentrations in the volcanic products decrease (Section 4.4). The lower As concentrations could be related to the change in the type of the assimilated crustal rocks of the basement, in which the shale-component (richer in As concentration; Bierlein et al., 2006) is less abundant. The pyroclastic centers within the Southern Puna preferably overlie rigid granitic-metamorphic basement (Guzmán et al., 2014) while granoitoids biotite gneiss-like, and gabbroic rocks are interpreted (through geochemical modeling) to dominate the composition of crustal materials assimilated by melts (Kay et al., 2010; Guzmán et al., 2011). These type of rocks generally contain lower As concentration (Table 1 and Welch et al., 1988; Smedley and Kinniburgh, 2002; Plant et al., 2014). Therefore, the lower As concentrations in comparison to the Northern Puna volcanic rocks maybe related to the assimilation of As depleted crustal rocks.

ii) Eruptive dynamics: in the previous section we have discussed the relationship between As content and magma composition. In this section we discuss how eruptive dynamics (highly influenced by magma composition) can influence As concentrations in volcanic deposits.

Generally, more silicic magmas lead to more explosive eruptions, which are those that can fragment the magma in smaller particles. During explosive volcanic eruptions pyroclasts, volcanic gases, and aerosols are liberated into the atmosphere forming (together with air) an eruption column. A large proportion of gas containing volatiles, such as As, maybe lost into the atmosphere by outgassing (Edmonds and Woods, 2018). In the Altiplano-Puna region As concentrations up to 1234 mg/L were measured in fumarolic gas of magmatic origin at 328 °C in the Lastarria stratovolcano (Aguilera et al., 2016).

During eruptions ashes play an important role in the sorption of volatiles phases (e.g. Ahmaruzzaman, 2010). Volatile As compounds can be sorbed onto ash particles, which are rich in highly reactive glass and have the smallest grain size and hence the largest surface area for reactions between permeating fluids and particles (e.g. Brown and Andrews, 2015). Several examples of As detected in volcanic ashes belong to eruptions such as Eyjafjallajökull volcano in Iceland, and Copahue, Lonquimay, Chaitén, Llaima, Puyehue, Hudson, Calbuco, and Cordón Caulle Volcanic Complex in the Southern Andes (Ruggieri et al., 2011; Ruggieri et al., 2012; Daga et al., 2014; Baccolo et al., 2015). Bia et al. (2015) measured As in volcanic ashes from Southern Andes volcanoes and found that As is mainly enriched in the surface of the ash particles forming sulfide or oxide compounds. In a recent work, Bia et al. (2022) also indicate that the concentration, speciation, and mobility of As in fresh Patagonian volcanic ash depend on the silica content of source magmas. The main As host in volcanic ash is Al-silicate glass and ashes have a trend of increasing As concentration with increasing silica (Bia et al., 2022). Gómez et al. (2002) measured the fractionation of As by particle size from the Copahue volcano ashes, describing As enrichment with decreasing grain size. Moreover, the finer particles are those which can reach the furthest distances from the emission centers. The extended Chaco-Pampean plain in Argentina is considered as one of the most important worldwide examples of high As concentrations in groundwater caused by the presence of rhyolitic ashes coming from distal Andean volcanic eruptions (Smedley et al., 2002; Nicolli et al., 2012). In eastern Patagonia, As concentrations in groundwaters of Peninsula de Valdez vary between 0.01 and 0.40 mg/L (Alvarez and Carol, 2019). This region is situated at >1000 km to the east of the Andean volcanic arc. Aquifer sediments are dominated by volcanic lithic fragments, volcanic glass shards and quartz, plagioclase, pyroxenes and magnetite clasts being the highest concentrations of As associated with volcanic shards and iron oxides (Alvarez and Carol, 2019). Considering that finer ashes are emitted from the most explosive eruptions and that high explosivity is usually observed in the most evolved compositions, it is expected that higher contents of As would be associated with fine ashes from intermediate to silicic compositions linked to highly explosive events.

In the Southern Puna, the correlation between eruptive dynamics, geochemical composition of the volcanic rocks, and particle sizes is observed at the Peinado stratovolcano (No. 55, Table 2, Fig. 2). Components from the most explosive eruptions of this volcano, i.e., pumices and ashes, are richer in As when compared to deposits generated by effusive eruptions. The rhyolitic pumice has the highest As concentration (69.6 mg/kg) within all the volcanic deposits. Next highest are rhyodacitic ashes (43.2 mg/kg) and trachyandesitic pumice (23.3 mg/kg); lavas have the lowest As concentrations (<0.5–6.7 mg/kg; data from Grosse et al., 2022). Calderas produced the most voluminous and thick deposits in the Altiplano-Puna plateau and consist of deposits of pyroclastic density currents (such as ignimbrites) and much less extensive fall deposits. Ignimbrites in the Altiplano-Puna contain one of the highest concentrations of As (Table 6) that may be favored by their formation after the development of low altitude eruptive columns or fountains that characterize many of the calderas of this region. Often, caldera collapses lead to very explosive eruptions with the development of high eruption columns that interact greatly with the atmosphere. However, most collapse calderas from the Altiplano-Puna plateau produce low eruptive columns in which the highly concentrated eruptive fountains out of the rim as highly concentrated pyroclastic density currents (e.g. Soler et al., 2007; Guzmán and Petrinovic, 2010; Guzmán et al., 2017c Guzmán et al., 2020; Petrinovic et al., 2021; Báez et al., 2020) that may be related to very high mass flow rate (Cas et al., 2011; Seggiaro et al., 2019) and relatively low velocity (Sulpizio et al., 2014; Guzmán et al., 2020). Thus, the possible explanation of why these ignimbrites contain high amounts of As is related to the persistent occurrence of these type of eruptions that produce dense pyroclastic density currents after the development of low altitude columns that do

not allow much air entrainment into the flow and hence efficiently maintain temperatures (e.g. Guzmán and Petrinovic, 2010) retaining As released from volatiles. Therefore, As released from volatiles may remain for longer time in the emplacing pyroclastic density currents and can be sorbed onto ash particles, resulting in deposits with a higher As concentration.

iii) Post-emplacement processes that enhance As enrichment of the deposits:

Exsolution of volatiles from the magmatic reservoirs that can lead to As enrichment in the previously erupted volcanic rocks, requires a continuous source of heat and volatiles and is therefore connected to the lifespan of a volcano, its size, and the depth of the magma. The lifespan of volcanoes is considered as the time interval between the oldest and youngest ages available for each volcano (Grosse et al., 2018). It is highly variable as a function of the type of volcanic edifice, which in turn are related to the size of the magma chambers feeding eruptions. Then, the higher lifespan and shallower position of magma chambers may be indicative of an active volcanic system that extends for a long period of time releasing volatiles and maintaining elevated temperatures around the vent area. An increasing magma chamber size is observed going from monogenetic volcanoes (in most cases directly linked to the magma generation source without temporal storage places), to stratovolcanoes (with lifespans that are particularly high in the central Andean volcanic arc, reaching 2 m. yr.; Grosse et al., 2018 and references therein), and collapse calderas. For the latter, lifespans of ca. 6 m. yr. were interpreted at the Cerro Galán Volcanic Complex (Kay et al., 2011) and 7 m. yr. for the Aguas Calientes caldera (Petrinovic et al., 2010). Regarding the correlation between magma chambers depth and types of volcanic edifices. Those that feed mafic monogenetic centers are usually very deep in the crust or even in the mantle (e.g. Martí et al., 2016; Fig. 6), even if some shallower-sourced magmas can also be involved (Smith and Németh, 2017). Depths of magma chambers that feed stratovolcanoes is highly variable from 5 to 20 km (Wörner et al., 2018; Fig. 6), while for collapse calderas magma chambers are usually located at relatively shallow depths (between 3 and 8 km depth for the Altiplano-Puna; e.g., de Silva and Kay, 2018 and references therein; Fig. 6). The continued exsolution of gases from magma chambers may be a very important source of As enrichment that feeds hydrothermal fluids and gases, altering previously erupted volcanic rocks during the non-eruptive phases. This relationship is evident in some volcanoes of the world, where non-altered and altered volcanic rocks show an extremely high difference in As concentrations (e.g. Fulignati et al., 1999). Accordingly, rhyolitic rocks with silicic alteration can have As concentrations of up to 1997 mg/kg while other samples from the same volcano show As contents as low as 3 mg/kg. This huge gradient indicates that the highly elevated As enrichment of volcanic rocks may be related to the non-explosive phases of a volcano's life. An exceptional example in the Altiplano-Puna is found at the Aguas Calientes caldera in which the non-altered ignimbrites have an As content of 12.5 mg/kg (No. 48; Table 2), while the altered ignimbrites hosting sulfide mineralization reach up to 7147 mg/kg of As (No. 49; Table 2).

5.2. Influence of volcanism on as enrichment in waters and sediments in the Altiplano-Puna

The volcanism in the Altiplano-Puna plateau strongly increases the As mobility in the upper crust and is a good example of a natural process enhancing As dispersion and availability in the hydrosphere (Nordstrom, 2012; Tapia et al., 2022). As mentioned in Section 1, As is found in all water types of the Altiplano-Puna plateau over a wide range of concentrations and in most cases the original source is related to the Cenozoic volcanism. For instance, sulfide veins emplaced in dacitic volcanic domes release high As concentration in acid rock drainages after the oxidation of sulfides such as As-rich pyrite, arsenopyrite, and other As reach sulfides from mining wastes (Murray et al., 2014, 2021; Sanci et al., 2020). In geothermal waters, As content is related to the leaching of volcanic rocks at high temperature (as described by Ellis and Mahon, 1964 and Ewers, 1977) by heated meteoric waters at depth (Peralta Arnold et al., 2017). In others volcanic centers such as Lastarria (Aguilera et al., 2016) the As concentrations in fumarolic vents could be associated to a mixture between meteoric and magmatic vapors as described by Valentino and Stanzione (2003). Once As is released from its volcanic sources, the distinctive characteristics of the region such as the semiarid climate, strong evaporation, the close basin hydrological systems, alkaline pH of waters, and predominance of Na-HCO_3 water types (due to competition of As with HCO_3 for adsorption sites in sediments) promotes high As concentrations in surface and groundwaters (e.g. Ormachea Muñoz et al., 2013, 2015, 2016; Murray et al., 2019; Tapia et al., 2022).

Regarding the As anomalies in the fluvial sediments of the Altiplano-Puna, they have a mean As content of 107 mg/kg (Table 2, Tapia et al., 2019), which is close to the mean value for the volcanic rocks of 96 mg/kg (considering altered and non-altered samples, Table 2). These values are around 20 times higher than the upper continental crust (4.8 mg/kg; Table 1; Rudnick and Gao, 2014) showing a considerable enrichment. Volcanic rocks cover a wide surface of the Altiplano-Puna plateau, ignimbrites outcrops situated mainly between 18° and 28°S, cover an area of 44,000 km^2, representing at least 10% of the surface (Petrinovic et al., 2010). For instance, stratovolcanoes in the Western Cordillera and southern Altiplano of Bolivia cover >24,000 km^2 (USGS and SGBO (U.S. Geological Survey and Servicio Geológico de Bolivia), 1975). Our calculation of the area covered by all type of Cenozoic volcanic rocks indicates approximately 108,554 km^2, which represents 22% of the total surface of the Altiplano-Puna (500,000 km^2). Therefore, volcanism could be considered as a regional As source that contributes to the regional anomaly of As in the sediments and waters.

The population in the Altiplano-Puna is in most cases affected by the presence of As in drinking water with values above the recommended limit (10 μg/L), especially in rural areas where access to good water quality is limited. An extraordinary example of how volcanism affects the As concentrations in water and the population of the region can be observed in the area of the COT lineament. The prime example is the San Antonio de los Cobres town where concentration of As in drinking water reached ≈ 200 μg/L (Concha et al., 1998; Concha et al., 2010; Hudson-Edwards and Archer, 2012; Sanci et al., 2020). Other examples in the Altiplano-Puna are described in (Tapia et al., 2019).

6. Conclusions

Volcanic rocks are the main regional source of geogenic As in waters in the Altiplano-Puna plateau. Arsenic concentrations in volcanic rocks without hydrothermal alteration present a mean value of 9.1 mg/kg which is almost 2 times higher than the upper continental crust. The As concentration in volcanic rocks increases with silica concentration, with the highest enrichments in dacites and rhyolites. Arsenic concentrations increases between different types of volcanic edifice from mafic (monogenetic centers as scoria cones and lava flows), toward intermediate (stratovolcanoes), and silicic (calderas and ignimbrite fields). The fact that peraluminous volcanic rocks show higher As concentration indicates that the assimilation of upper crustal rocks such as sedimentary rocks and especially shale-type sediments are an important source of As to the magmas. In comparison to other volcanic zones in the Andean arc, crustal assimilation is enhanced in the Central Volcanic Zone of the Andes and therefore in the Altiplano-Puna plateau because the crust is extremely thick (up to >70 km), favoring the development of large magma bodies where significant MASH process takes place. A possible explanation for the high As concentration in deposits of pyroclastic density currents derived from collapse calderas of the Altiplano-Puna is their common origin from low-eruption columns. These types of eruptions may hinder an easy release of volatiles to the atmosphere (a portion of them is trapped in the dense pyroclastic density currents) and favor their retention during compaction and cooling of pyroclastic

deposits, further enriching them with As.

Hydrothermal alteration and sulfide mineralization are also important post-emplacement processes that increase the As content in volcanic rocks from continued input of As-rich volatiles sourced from underlying magmatic systems and/or transfer of As in hydrothermal systems. Hydrothermal alteration and sulfide mineralization increase up to 100 times the As enrichment in volcanic rocks (957 mg/kg).

The presence of regional structures and lineaments acting as zones of tectonic transfer for magmas and hydrothermal fluids circulation such as in the COT lineament enhance the transfer of As from the enriched melts to the surface, and therefore to different type of waters and nearby population.

The Cenozoic volcanism in the Altiplano-Puna plateau favors As availability in the upper the crust and the dispersion in the interface with the hydrosphere. Coupled with the intrinsic characteristics of the region such as strong evaporation, closed basin hydrology, alkaline pH, and Na-HCO_3 water type, the As anomaly is highly enhanced making of this a strongly As enriched region in the world. Groundwaters in the region should be tested and treated for geogenic As (and potential B, Cs, F, and Li) before being used as drinking water supply.

Declaration of Competing Interest

The authors declare that they have no known competing financial interests or personal relationships that could have appeared to influence the work reported in this paper.

Data availability

Data will be made available on request.

Acknowledgments

The authors acknowledge to the IGCP-707 (UNESCO-IUGS) project that provided the framework for collaboration and to Fondecyt 11180090 from the National Agency of Investigation and Development of Chile (ANID). The support of the U.S. Geological Survey is acknowledged; we particularly thank Lauren Harrison for her revisions that helped to improve our manuscript. Any use of trade, firm, or product names is for descriptive purposes only and does not imply endorsement by the U.S. Government. The authors gratefully acknowledge Brandon Schneider for English support and discussions. Revisions provided by Prof. Karoly Nemeth and other two anonymous reviewers significantly contributed to ameliorate our manuscript. We acknowledge Carolina Montero for sharing arsenic unpublished data as well as data published on her PhD thesis (Montero-López, 2009).

Appendix A. Supplementary data

The Supplementary Material is composed of: A Glossary to define terms used within volcanism vocabulary. Terms and definitions were taken mainly from Sigurdsson et al. (2015). A Table (Table S1) with the research compiled data for this publication. Supplementary data to this article can be found online at https://doi.org/10.1016/j.chemgeo.2023.121473.

References

Acocella, V., Gioncada, A., Omarini, R., Riller, U., Mazzuoli, R., Vezzoli, L., 2011. Tectonomagmatic characteristics of the back-arc portion of the Calama–Olacapato–El Toro fault zone, Central Andes. Tectonics 30, 77–94. https://doi.org/10.1029/2010TC002854.

Aguilera, F., Layana, S., Rodríguez-Díaz, A., González, C., Cortés, J., Inostroza, M., 2016. Alteración hidrotermal, depósitos fumarólicos y fluidos del Complejo Volcánico Lastarria: Un estudio multidisciplinario. Andean Geol. 43, 166–196. https://doi.org/10.5027/andgeoV43n2-a02.

Ahmaruzzaman, M., 2010. A review on the utilization of fly ash. Prog. Energy Combust. Sci. 36, 327–363. https://doi.org/10.1016/j.pecs.2009.11.003.

Aiuppa, A., D'Alessandro, W., Federico, C., Palumbo, B., Valenza, M., 2003. The aquatic geochemistry of arsenic in volcanic groundwaters from southern Italy. Appl. Geochem. 18, 1283–1296. https://doi.org/10.1016/S0883-2927(03)00051-9.

Aiuppa, A., Avino, R., Brusca, L., Caliro, S., Chiodini, G., D'Alessandro, W., Favara, R., Federico, C., Ginevra, W., Inguaggiato, S., Longo, M., Pecoraino, G., Valenza, M., 2006. Mineral control of arsenic content in thermal waters from volcano-hosted hydrothermal systems: Insights from island of Ischia and Phlegrean Fields (Campanian Volcanic Province, Italy). Chem. Geol. 229, 313–330. https://doi.org/10.1016/j.chemgeo.2005.11.004.

Alarcón-Herrera, M.T., Martin-Alarcon, D.A., Gutiérrez, M., Reynoso-Cuevas, L., Martín-Domínguez, A., Olmos-Márquez, M.A., Bundschuh, J., 2020. Co-occurrence, possible origin, and health-risk assessment of arsenic and fluoride in drinking water sources in Mexico: Geographical data visualization. Sci. Total Environ. 698, 134168 https://doi.org/10.1016/j.scitotenv.2019.134168.

Allmendinger, R.W., 1986. Tectonic development, southeastern border of the Puna Plateau, northwestern argentine Andes. GSA Bull. 97, 1070–1082. https://doi.org/10.1130/0016-7606(1986)97b1070:TDSBOTN2.0.CO;2.

Allmendinger, R., Jordan, T., Kay, S., Isacks, B.L., 1997. The evolution of the Altiplano-Puna plateau of the Central Andes. Annu. Rev. Earth Planet. Sci. 25, 139–174. https://doi.org/10.1146/annurev.earth.25.1.139.

Alonso, R., Viramonte, J., Gutierrez, R., 1984. Puna Austral. Bases para el subprovincialismo geológico de la Puna argentina. In: Noveno Congreso Geológico Argentino Proceedings, pp. 43–63.

Alonso, R.N., Jordan, T.E., Tabbutt, K.T., Vandervoort, D.S., 1991. Giant evaporite belts of the Neogene central Andes. Geology 19, 401–404. https://doi.org/10.1130/0091-7613(1991)019b0401:GEBOTNN2.3.CO;2.

Alvarez, M.P., Carol, E., 2019. Geochemical occurrence of arsenic, vanadium and fluoride in groundwater of Patagonia, Argentina: sources and mobilization processes. J. S. Am. Earth Sci. 89, 1–9. https://doi.org/10.1016/j.jsames.2018.10.006.

Angelone, M., Cremisini, C., Piscopo, V., Proposito, M., Spaziani, F., 2009. Influence of hydrostratigraphy and structural setting on the arsenic occurrence in groundwater of the Cimino-Vico volcanic area (Central Italy). Hydrogeol. J. 17, 901–914. https://doi.org/10.1007/s10040-008-0401-3.

Aramayo, A., Guzmán, S., Hongn, F., del Papa, C., Montero-López, C., Sudo, M., 2017. A Middle Miocene (13.5–12 Ma) deformational event constrained by volcanism along the Puna-Eastern Cordillera border, NW Argentina. Tectonophysics 703–704, 9–22. https://doi.org/10.1016/j.tecto.2017.02.018.

Baccolo, G., Clemenza, M., Delmonte, B., Maffezzoli, N., Nastasi, M., Previtali, E., Maggi, V., 2015. Assessing the geochemical fingerprint of the 2010 Eyjafjallajökull tephra through instrumental neutron activation analysis: a trace element approach. J. Radioanal. Nucl. Chem. 306, 429–435. https://doi.org/10.1007/s10967-015-4092-7.

Báez, W., de Silva, S., Chiodi, A., Bustos, E., Giordano, G., Arnosio, M., Suzaño, N., Viramonte, J.G., Norini, G., Gropelli, G., 2020. Pulsating Flow dynamics of sustained, forced pyroclastic density currents: insights from a facies analysis of the Campo de la Piedra Pómez ignimbrite, southern Puna, Argentina. Bulletin of Volcanology 82, 53. https://doi.org/10.1007/s00445-020-01385-5.

Bardelli, L., Becchio, R., Ortíz, A., Schmitt, A.K., Pereira, R., Báez, W., Reckziegel, F., Viramonte, L., Giordano., G., 2021. Repeated extraction of aphyric melts in a rhyolitic system revealed by zircon age and composition: the Ramadas Volcanic Centre (Puna plateau), NW Argentina. Lithos 392, 106141. https://doi.org/10.1016/j.lithos.2021.106141.

Best, M.G., Christiansen, E., Silva, S., Lipman, P.W., 2016. Slab-rollback ignimbrite flareups in the southern Great Basin and other Cenozoic American arcs: a distinct style of arc volcanism. Geosphere 12 (4), 1097–1135. https://doi.org/10.1130/GES01285.1.

Bia, G., Borgnino, L., Gaiero, D., García, M.G., 2015. Arsenic-bearing phases in South Andean volcanic ashes: Implications for As mobility in aquatic environments. Chem. Geol. 393–394, 26–35. https://doi.org/10.1016/j.chemgeo.2014.10.007.

Bia, G., García, M.G., Cosentino, N.J., Borgnino, L., 2022. Dispersion of arsenic species from highly explosive historical volcanic eruptions in Patagonia. Sci. Total Environ. 853, 158389. https://doi.org/10.1016/j.scitotenv.2022.158389.

Bianchi, M., Heit, B., Jakovlev, A., Yuan, X., Kay, S.M., Sandvol, E., Alonso, R.N., Coira, B., Brown, L., Kind, R., Comte, D., 2013. Teleseismic tomography of the southern Puna plateau in Argentina and adjacent regions. Tectonophysics 586, 65–83. https://doi.org/10.1016/j.tecto.2012.11.016.

Bianchini, G., Brombin, V., Marchina, C., Natali, C., Godebo, T.R., Rasini, A., Salani, G. M., 2020. Origin of fluoride and arsenic in the main ethiopian rift waters. Minerals 10. https://doi.org/10.3390/min10050453.

Bierlein, F.P., Stein, H.J., Coira, B., Reynolds, P., 2006. Timing of gold and crustal evolution of the Palaeozoic south Central Andes, NW Argentina-implications for the endowment of orogenic belts. Earth Planet. Sci. Lett. 245, 702–721. https://doi.org/10.1016/j.epsl.2006.03.019.

Bird, P., 2003. An updated digital model of plate boundaries. Geochem. Geophys. Geosyst. 4, 1027. https://doi.org/10.1029/2001GC000252.

Borisova, A.Y., Pokrovski, G.S., Pichavant, M., Freydier, R., Candaudap, F., 2010. Arsenic enrichment in hydrous peraluminous melts: Insights from femtosecond laser ablation-inductively coupled plasma-quadrupole mass spectrometry, and in situ X-ray absorption fine structure spectroscopy. Am. Mineral. 95, 1095–1104. https://doi.org/10.2138/am.2010.3424.

Bowell, R.J., Alpers, Ch.N., Jamieson, H.E., Nordstrom, D.K., Majzlan, J., 2014. The environmental geochemistry of arsenic — an overview. In: Bowell, R.J., Alpers, C.N., Jamieson, H.E., Nordstrom, D.K., Majzlan, J. (Eds.), Reviews in Mineralogy and Geochemistry, Arsenic: Environmental Geochemistry, Mineralogy, and Microbiology, 79, pp. 1–16. https://doi.org/10.2138/rmg.2014.79.1.

Brown, R.J., Andrews, G.D., 2015. Deposits of pyroclastic density currents. In: *The encyclopedia of volcanoes*. Academic Press, pp. 631–648.
Cas, R.A., Wright, H.M., Folkes, C.B., Lesti, C., Porreca, M., Giordano, G., Viramonte, J. G., 2011. The flow dynamics of an extremely large volume pyroclastic flow, the 2.08-Ma Cerro Galán Ignimbrite, NW Argentina, and comparison with other flow types. Bull. Volcanol. 73, 1583–1609. https://doi.org/10.1007/s00445-011-0564-y.
Cinti, D., Poncia, P.P., Brusca, L., Tassi, F., Quattrocchi, F., Vaselli, O., 2015. Spatial distribution of arsenic, uranium and vanadium in the volcanic-sedimentary aquifers of the Vicano-Cimino Volcanic District (Central Italy). J. Geochem. Explor. 152, 123–133. https://doi.org/10.1016/j.gexplo.2015.02.008.
Cinti, D., Vaselli, O., Poncia, P.P., Brusca, L., Grassa, F., Procesi, M., Tassi, F., 2019. Anomalous concentrations of arsenic, fluoride and radon in volcanic-sedimentary aquifers from Central Italy: Quality indexes for management of the water resource. Environ. Pollut. 253, 525–537. https://doi.org/10.1016/j.envpol.2019.07.063.
Coira, B., Kay, S.M., Viramonte, J.G., Kay, R.W., Galli, C., 2018. Origin of late Miocene Peraluminous Mn-rich Garnet-bearing Rhyolitic Ashes in the Andean Foreland (Northern Argentina). J. Volcanol. Geotherm. Res. 364, 20–34. https://doi.org/10.1016/j.jvolgeores.2018.08.020.
Concha, G., Nermell, B., Vahter, M., 1998. Metabolism of inorganic arsenic in children with chronic high arsenic exposure in northern Argentina. Environ. Health Perspect. 106 (6), 355–359. https://doi.org/10.1289/ehp.98106355.
Concha, G., Broberg, K., Grandér, M., Cardozo, A., Palm, B., Vahter, M., 2010. High level exposure to lithium, boron, cesium, and arsenic via drinking water in the Andes of northern Argentina. Environ. Sci. Technol. 44, 6875–6880. https://doi.org/10.1021/es1010384.
Condesso de Melo, M.T., Shandilya, R.N., Silva, J.B.P., Postma, D., 2020. Volcanic glass leaching and the groundwater geochemistry on the semi-arid Atlantic island of Porto Santo. Appl. Geochem. 114, 1–12. https://doi.org/10.1016/j.apgeochem.2019.104470.
Daga, R., Ribeiro Guevara, S., Poire, D.G., Arribére, M., 2014. Characterization of tephras dispersed by the recent eruptions of volcanoes Calbuco (1961), Chaitén (2008) and Cordón Caulle Complex (1960 and 2011), in Northern Patagonia. J. S. Am. Earth Sci. 49, 1–14. https://doi.org/10.1016/j.jsames.2013.10.006.
de Silva, S.L., Kay, S.M., 2018. Turning up the heat: high-flux magmatism in the Central Andes. Elements: an International Magazine of Mineralogy. Geochemistry, and Petrology 14, 245–250. https://doi.org/10.2138/gselements.14.4.245.
de Silva, S.L., Riggs, N.R., Barth, A.P., 2015. Quickening the pulse: fractal tempos in continental arc magmatism. Elements 11, 113–118. https://doi.org/10.2113/gselements.11.2.113.
Edmonds, M., Woods, A.W., 2018. Exsolved volatiles in magma reservoirs. J. Volcanol. Geotherm. Res. 368, 13–30. https://doi.org/10.1016/j.jvolgeores.2018.10.018.
Ellis, A.J., Mahon, W.A.J., 1964. Natural hydrothermal systems and experimental hot-water/rock interactions. Geochim. Cosmochim. Acta 28, 1323–1357. https://doi.org/10.1016/0016-7037(64)90132-2.
Ewers, G.R., 1977. Experimental hot water-rock interactions and their significance to natural hydrothermal systems in New Zealand. Geochim. Cosmochim. Acta 41, 143–150. https://doi.org/10.1016/0016-7037(77)90194-6.
Filipovich, R., Chiodi, A., Báez, W., Ahumada, M.F., Invernizzi, C., Taviani, S., et al., 2022. Structural analysis and fluid geochemistry as tools to assess the potential of the Tocomar geothermal system, Central Puna (Argentina). Geothermics 98, 102297. https://doi.org/10.1016/j.geothermics.2021.102345.
Flanagan, F.J., 1976. Descriptions and Analyses of Eight New USGS Rock Standards, pp. 171–172.
Francis, P.W., Baker, M.C.W., 1978. Sources of two large volume ignimbrites in the Central Andes: some Landsat evidence. J. Volcanol. Geotherm. Res. 4, 81–87. https://doi.org/10.1016/0377-0273(78)90029-X.
Fulignati, P., Gioncada, A., Sbrana, A., 1999. Rare-earth element (REE) behaviour in the alteration facies of the active magmatic–hydrothermal system of Vulcano (Aeolian Islands, Italy). J. Volcanol. Geotherm. Res. 88 (4), 325–342. https://doi.org/10.1016/S0377-0273(98)00117-6.
Giordano, G., Pinton, A., Cianfarra, P., Baez, W., Chiodi, A., Viramonte, J., Norini, G., Groppelli, G., 2013. Structural control on geothermal circulation in the Cerro Tuzgle–Tocomar geothermal volcanic area (Puna plateau, Argentina). J. Volcanol. Geotherm. Res. 249, 77–94. https://doi.org/10.1016/j.jvolgeores.2012.09.009.
Gómez, D., Smichowski, P., Polla, G., Ledesma, A., Resnizky, S., Rosa, S., 2002. Fractionation of elements by particle size of ashes ejected from Copahue Volcano, Argentina. J. Environ. Monit. 4, 972–977. https://doi.org/10.1039/b207080b.
Gorustovich, S., Vullien, A., Aniel, B., Bustos, R., 1989. Uranio en relación a ignimbritas Cenozoicas de la comarca Coranzuli-Ramallo, Puna Argentina. Asociación Geológica Argentina Revista 44, 175–185.
Gregory-Wodzicki, K.M., 2000. Uplift history of the Central and Northern Andes: a review. Geol. Soc. Am. Bull. 112 (7), 1091–1105. https://doi.org/10.1130/0016-7606(2000)112%3C1091:UHOTCA%3E2.0.CO;2.
Grosse, P., Guzmán, S., 2017. Volcanismo. In: Grau, H.R., Babot, M.J., Izquierdo, A.E., Grau, A. (Eds.), La Puna Argentina: Naturaleza y Cultura, Conservación, 24. Fundación Miguel Lillo, pp. 32–51. https://ri.conicet.gov.ar/handle/11336/129419.
Grosse, P., Orihashi, Y., Guzmán, S.R., Sumino, H., Nagao, K., 2018. Eruptive history of Incahuasi, Falso Azufre and El Cóndor Quaternary composite volcanoes, southern Central Andes. Bull. Volcanol. 80, 1–26. https://doi.org/10.1007/s00445-018-1221-5.
Grosse, P., Guzmán, S.R., Nauret, F., Orihashi, Y., Sumino, H., 2022. Central vs. lateral growth evolution at the potentially active Quaternary Peinado composite volcano, southern Central Volcanic Zone of the Andes. J. Volcanol. Geotherm. Res. 425, 107532 https://doi.org/10.1016/j.jvolgeores.2022.107532.
Guzmán, S., Petrinovic, I., 2010. The Luingo caldera: the south-easternmost collapse caldera in the Altiplano–Puna plateau, NW Argentina. J. Volcanol. Geotherm. Res. 194, 174–188. https://doi.org/10.1016/j.jvolgeores.2010.05.009.
Guzmán, S., Petrinovic, I.A., Brod, J.A., Hongn, F.D., Seggiaro, R.E., Montero, C., Carniel, R., Dantas, E.L., Sudo, M., 2011. Petrology of the Luingo caldera (SE margin of the Puna plateau): a middle Miocene window of the arc-back arc configuration. J. Volcanol. Geotherm. Res. 200, 171–191. https://doi.org/10.1016/j.jvolgeores.2010.12.008.
Guzmán, S., Grosse, P., Montero-López, C., Hongn, F., Pilger, R., Petrinovic, I., Seggiaro, R., Aramayo, A., 2014. Spatial-temporal distribution of explosive volcanism in the 25-28°S segment of the Andean Central Volcanic Zone. Tectonophysics 636, 170–189. https://doi.org/10.1016/j.tecto.2014.08.013.
Guzmán, S., Neri, M., Carniel, R., Martí, J., Grosse, P., Montero-López, C., Geyer, A., 2017a. Remarkable variability in dyke features at the Vicuña Pampa Volcanic complex, Southern Central Andes. Terra Nova 29, 224–232. https://doi.org/10.1111/ter.12268.
Guzmán, S., Strecker, M.R., Martí, J., Petrinovic, I.A., Schildgen, T.F., Grosse, P., Montero-López, C., Neri, M., Carniel, R., Hongn, F.D., Muruaga, C., Sudo, M., 2017b. Construction and degradation of a broad volcanic massif: the Vicuña pampa volcanic complex, southern Central Andes, NW Argentina. Bull. Geol. Soc. Am. 129, 750–766. https://doi.org/10.1130/B31631.1.
Guzmán, S., Grosse, P., Martí, J., Petrinovic, I.A., Seggiaro, R., 2017c. Calderas cenozoicas argentinas de la Zona Volcánica Central de los Andes – procesos eruptivos y dinámica: una revisión: 518-547. In: Muruaga, C., Grosse, P. (Eds.), 2017. Ciencias de la Tierra y Recursos Naturales del NOA. Relatorio del XX Congreso Geológico Argentino, San Miguel de Tucumán, 1194 (pp. ISBN: 978-987-42-6666-8).
Guzmán, S., Doronzo, D.M., Martí, J., Seggiaro, R., 2020. Characteristics and emplacement mechanisms of the Coranzulí ignimbrites (Central Andes). Sediment. Geol. 405, 105699 https://doi.org/10.1016/j.sedgeo.2020.105699.
Hedenquist, J.W., Lowenstern, J.B., 1994. The role of magmas in the formation of hydrothermal ore deposits. Nature 370, 519–527. https://doi.org/10.1038/370519a0.
Hildreth, W., Moorbath, S., 1988. Crustal contributions to arc magmatism in the Andes of Central Chile. Contrib. Mineral. Petrol. 98, 455–489. https://doi.org/10.1007/BF00372365.
Hu, Z., Gao, S., 2008. Upper crustal abundances of trace elements: a revision and update. Chem. Geol. 253 (3–4), 205–221. https://doi.org/10.1016/j.chemgeo.2008.05.010.
Hudson-Edwards, K.A., Archer, J., 2012. Geochemistry of As- F- and B-bearing waters in and around San Antonio de los Cobres, Argentina, and implications for drinking and irrigation water quality. J. Geochem. Explor. 112, 276–284. https://doi.org/10.1016/j.gexplo.2011.09.007.
Igarzábal, A., 1999. Cuaternario de la Puna (Geología Argentina No. Anales 29). Instituto de Geología y Recursos Minerales, Servicio Geológico Minero Argentino, Buenos Aires, Argentina.
IRIS (Integrated Risk Information System), 1991. Arsenic, Inorganic: CASRN 7440-38-2.
Kay, S.M., Coira, B.L., 2009. Shallowing and steepening subduction zones, continental lithospheric loss, magmatism, and crustal flow under the Central Andean Altiplano-Puna Plateau. In: Kay, S.M., Ramos, V.A., Dickinson, W.R. (Eds.), Backbone of the Americas: Shallow Subduction, Plateau Uplift, and Ridge and Terrane Collision. https://doi.org/10.1130/2009.1204(11).
Kay, S.M., Coira, B.L., Caffe, P.J., Chen, C.-H., 2010. Regional chemical diversity, crustal and mantle sources and evolution of central Andean Puna plateau ignimbrites. J. Volcanol. Geotherm. Res. 198, 81–111. https://doi.org/10.1016/j.jvolgeores.2010.08.013.
Kay, S.M., Coira, B., Wörner, G., Kay, R.W., Singer, B.S., 2011. Geochemical, isotopic and single crystal 40Ar/39Ar age constraints on the evolution of the Cerro Galán ignimbrites. Bull. Volcanol. 73, 1487–1511. https://doi.org/10.1007/s00445-010-0410-7.
Kirschbaum, A., Murray, J., Arnosio, M., Tonda, R., Cacciabue, L., 2012. Pasivos ambientales mineros en el noroeste de Argentina: aspectos mineralógicos, geoquímicos y consecuencias ambientales. Revista Mexicana de Ciencias Geológicas 29 (1), 248–264.
LaFemina, P.C., 2015. Plate Tectonics and Volcanism. The Encyclopedia of Volcanoes. https://doi.org/10.1016/B978-0-12-385938-9.00003-1.
Lamb, S., Hoke, L., 1997. Origin of the high plateau in the Central Andes, Bolivia, South America. Tectonics 16, 623–649. https://doi.org/10.1029/97TC00495.
Lanza, F., Tibaldi, A., Bonali, F.L., Corazzato, C., 2013. Space–time variations of stresses in the Miocene–Quaternary along the Calama–Olacapato–El Toro fault zone, Central Andes. Tectonophysics 593, 33–56. https://doi.org/10.1016/j.tecto.2013.02.029.
Le Bas, M.J., Streckeisen, A.L., 1991. The IUGS systematics of igneous rocks. J. Geol. Soc. 148 (5), 825–833. https://doi.org/10.1144/gsjgs.148.5.0825.
Le Maitre, et al., 1989. A Classification of Igneous Rocks and Glossary of Terms. Blackwell, Oxford.
López, D.L., Bundschuh, J., Birkle, P., Armienta, M.A., Cumbal, L., Sracek, O., Cornejo, L., Ormachea, M., 2012. Arsenic in volcanic geothermal fluids of Latin America. Sci. Total Environ. 429, 57–75. https://doi.org/10.1016/j.scitotenv.2011.08.043.
Lucci, F., Rossetti, F., Becchio, R., Theye, T., Gerdes, A., Opitz, J., Baez, W., Bardelli, L., De Astis, G., Viramonte, J., Giordano, G., 2018. Magmatic Mn-rich garnets in volcanic settings: Age and longevity of the magmatic plumbing system of the Miocene Ramadas volcanism (NW Argentina). Lithos 322, 238–249. https://doi.org/10.1016/j.lithos.2018.10.016.
Mahlknecht, J., Steinich, B., Navarro De León, I., 2004. Groundwater chemistry and mass transfers in the Independence aquifer, central Mexico, by using multivariate statistics and mass-balance models. Environ. Geol. 45, 781–795. https://doi.org/10.1007/s00254-003-0938-3.

Martí, J., López, C., Bartolini, S., Becerril, L., Geyer, A., 2016. Stress controls of monogenetic volcanism: a review. Front. Earth Sci. 4 https://doi.org/10.3389/feart.2016.00106.

Mattioli, M., Renzulli, A., Menna, M., Holm, P.M., 2006. Rapid ascent and contamination of magmas through the thick crust of the CVZ (Andes, Ollagüe region): evidence from a nearly aphyric high-K andesite with skeletal olivines. J. Volcanol. Geotherm. Res. 158, 87–105. https://doi.org/10.1016/j.jvolgeores.2006.04.019.

Montero-Lápez, M.C., Hongn, F., Marrett, R., Seggiaro, R., Strecker, M., Sudo, M., 2010. Late MioceneePliocene onset of N-S extension along the southern margin of the Central Andean Puna plateau from magmatic, geochronological and structural evidences. Tectonophysics 494, 48–63. https://doi.org/10.1016/j.tecto.2010.08.010.

Montero-López, M.C., 2009. Estructura y magmatismo Neógeno-Cuaternarios en la Sierra de San Buenaventura (Catamarca): su vinculación con la terminación austral de la Puna. PhD Thesis. Universidad Nacional de Salta, Argentina (255 p).

Montero-López, M.C., Hongn, F., Brod, J.A., Seggiaro, R., Marrett, R., Sudo, M., 2010. Magmatismo ácido del Mioceno Superior-Cuaternario en el área de Cerro Blanco-La Hoyada, Puna Sur. Rev. Asoc. Geol. Argent. 67 (3), 329–348.

Montero-López, C., Guzmán, S., Hongn, F., 2011. Ignimbritas de la Quebrada del Río Las Papas (Cordillera de San Buenaventura, Catamarca): una primera aproximación petrológica y geoquímica. Acta Geol. Lilloana 23 (1–2), 78–93.

Montero-López, C., Guzmán, S., Barrios, F., 2015. Late Miocene ignimbrites at the southern Puna–northern Sierras Pampeanas border (~27°S): stratigraphic correlation. J. S. Am. Earth Sci. 62, 80–91. https://doi.org/10.1016/j.jsames.2015.05.004.

Morales, I., Villanueva-Estrada, R.E., Rodríguez, R., Armienta, M.A., 2015. Geological, hydrogeological, and geothermal factors associated to the origin of arsenic, fluoride, and groundwater temperature in a volcanic environment “El Bajío Guanajuatense”, Mexico. Environ. Earth Sci. 74, 5403–5415. https://doi.org/10.1007/s12665-015-4554-9.

Morales-Simfors, N., Bundschuh, J., Herath, I., Inguaggiato, C., Caselli, A.T., Tapia, J., Choquehuayta, F.E.A., Armienta, M.A., Ormachea, M., Joseph, E., López, D.L., 2020. Arsenic in Latin America: a critical overview on the geochemistry of arsenic originating from geothermal features and volcanic emissions for solving its environmental consequences. Sci. Total Environ. 716 https://doi.org/10.1016/j.scitotenv.2019.135564.

Mukherjee, A., Gupta, S., Coomar, P., Fryar, A.E., Guillot, S., Verma, S., Bhattacharya, P., Bundschuh, J., Charlet, L., 2019. Plate tectonics influence on geogenic arsenic cycling: from primary sources to global groundwater enrichment. Sci. Total Environ. 683, 793–807. https://doi.org/10.1016/j.scitotenv.2019.04.255.

Murcia, H., Németh, K., 2020. Effusive monogenetic volcanism. In *Updates in Volcanology-Transdisciplinary Nature of Volcano Science*. IntechOpen.

Murray, J., Kirschbaum, A., Dold, B., Mendes, Guimaraes E., Pannunzio, Miner E., 2014. Jarosite versus Soluble iron-sulfate formation and their role in acid mine drainage formation at the Pan de Azúcar Mine tailings (Zn-Pb-Ag). NW Argentina. Minerals 4 (2), 477–502. https://doi.org/10.3390/min4020477.

Murray, J., Nordstrom, D.K., Dold, B., Romero Orué, M., Kirschbaum, A., 2019. Origin and geochemistry of arsenic in surface and groundwaters of Los Pozuelos basin, Puna region, Central Andes, Argentina. Science of the Total Environment 697. https://doi.org/10.1016/j.scitotenv.2019.134085.

Murray, J., Nordstrom, D.K., Dold, B., Kirschbaum, A., 2021. Seasonal fluctuations and geochemical modeling of acid mine drainage in the semi-arid Puna region: the Pan de Azúcar Pb-Ag-Zn mine, Argentina. J. S. Am. Earth Sci. 109, 103197 https://doi.org/10.1016/j.jsames.2021.103197.

Neff, J.M., 2002. Bioaccumulation in marine organisms: effect of contaminants from oil well produced water, 451. Elsevier.

Nicolli, H.B., Bundschuh, J., Blanco, C., Tujchneider, O.C., Panarello, H.O., Dapeña, C., Rusansky, J.E., 2012. Arsenic and associated trace-elements in groundwater from the Chaco-Pampean plain, Argentina: results from100 years of research. Sci. Total Environ. 429, 36–56. https://doi.org/10.1016/j.scitotenv.2012.04.048.

Nordstrom, D.K., 2002. Worldwide occurrences of arsenic in ground water. Science 296, 2143–2145. https://doi.org/10.1126/science.1072375.

Nordstrom, D.K., 2012. Arsenic in the geosphere meets the anthroposphere. In: Ng, J., Noller, B., Naidu, R., Bundschuh, J., Bhattacharya, P. (Eds.), Understanding the Geological and Medical Interface of Arsenic. Proceedings of the 4th International Congress on Arsenic in the Environment, 22-27 July 2012, Cairns, Australia. Taylor and Francis, London, pp. 15–19. https://doi.org/10.1201/b12522.

Norini, G., Baez, W., Becchio, R., Viramonte, J., Giordano, G., Arnosio, M., Pinton, A., Groppelli, G., 2013. The Calama–Olacapato–El Toro fault system in the Puna Plateau, Central Andes: Geodynamic implications and stratovolcanoes emplacement. Tectonophysics 608, 1280–1297. https://doi.org/10.1016/j.tecto.2013.06.013.

Ormachea Muñoz, M., Wern, H., Johnsson, F., Bhattacharya, P., Sracek, O., Thunvik, R., Quintanilla, J., Bundschuh, J., 2013. Geogenic arsenic and other trace elements in the shallow hydrogeologic system of Southern Poopó Basin, Bolivian Altiplano. J. Hazard. Mater. 262, 924–940. https://doi.org/10.1016/j.jhazmat.2013.06.078.

Ormachea Muñoz, M., Bhattacharya, P., Šráček, O., Ramos, R., Quintanilla Aguirre, J., Bundschuh, J., Maity, J.P.R., 2015. Arsenic and other trace elements in thermal springs and in cold waters from drinking water wells on the Bolivian Altiplano. J. S. Am. Earth Sci. 60, 10–20. https://doi.org/10.1016/j.jsames.2015.02.006.

Ormachea Muñoz, M., Aróstegui, J.L.G., Bhattacharya, P., Sracek, O., Moreno, M.E.G., Kohfahl, C., Aguirre, J.Q., Diaz, J.H., Bundschuh, J., 2016. Geochemistry of naturally occurring arsenic in groundwater and surface-water in the southern part of the Poopó Lake basin, Bolivian Altiplano. Groundw. Sustain. Dev. 2, 104–116. https://doi.org/10.1016/j.gsd.2016.04.002.

Palme, H., O’Neill, H.St.C., 2014. Cosmochemical estimates of mantle composition. In: Holland, Heinrich D., Turekian, Karl K. (Eds.), Treatise on Geochemistry (Second Edition). Elsevier, pp. 1–39. https://doi.org/10.1016/B978-0-08-095975-7.00201-1.

Peralta Arnold, Y., Cabassi, J., Tassi, F., Caffe, P.J., Vaselli, O., 2017. Fluid geochemistry of a deep-seated geothermal resource in the Puna plateau (Jujuy Province, Argentina). J. Volcanol. Geotherm. Res. 338, 121–134. https://doi.org/10.1016/j.jvolgeores.2017.03.030.

Perkins, J.P., Ward, K.M., De Silva, S.L., Zandt, G., Beck, S.L., Finnegan, N.J., 2016. Surface uplift in the Central Andes driven by growth of the Altiplano Puna Magma Body. Nat. Commun. 7, 1–10. https://doi.org/10.1038/ncomms13185.

Petrinovic, I.A., Mitjavila, J., Viramonte, J.G., Marti, J., Becchio, R., Arnosio, M., Colombo, F., 1999. Descripción geoquímica y geocronológica de secuencias volcánicas neógenas de trasarco, en el extremo oriental de la cadena volcánica transversal del Quevar (Noroeste de Argentina). Acta Geologica Hispanica 34, 255–272.

Petrinovic, I.A., Riller, U., Brod, J.A., Alvarado, G., Arnosio, M., 2006. Bimodal volcanism in a tectonic transfer zone: evidence for tectonically controlled magmatism in the southern Central Andes, NW Argentina. J. Volcanol. Geotherm. Res. 152, 240–252. https://doi.org/10.1016/j.jvolgeores.2005.10.008.

Petrinovic, I.A., Martí, J., Aguirre-Díaz, G.J., Guzmán, S., Geyer, A., Paz, N.S., 2010. The Cerro Aguas Calientes caldera, NW Argentina: an example of a tectonically controlled, polygenetic collapse caldera, and its regional significance. J. Volcanol. Geotherm. Res. 194, 15–26. https://doi.org/10.1016/j.jvolgeores.2010.04.012.

Petrinovic, I.A., Hernando, I.R., Guzmán, S.R., 2021. Miocene to recent collapse calderas of the southern and central volcanic zones of the Andes and their tectonic constraints. International Journal of Earth Sciences. https://doi.org/10.1007/s00531-020-01974-x. Springer Berlin Heidelberg.

Plant, J.A., Bone, J., Voulvoulis, N., Kinniburgh, D.G., Smedley, P.L., Fordyce, F.M., Klinck, B., 2014. Chapter 11.2: Arsenic and Selenium. In: Sherwood Lollar, B. (Ed.), Environmental Geochemistry. Holland H D and Turekian K K. (Exec Editors) Treatise on Geochemistry, , Second editionvol. 11. Elsevier, Oxford, pp. 13–57. https://doi.org/10.1016/B978-0-08-095975-7.00902-5.

Ramellow, J., Riller, U., Romer, R.L., Oncken, O., 2006. Kinematic link between episodic trapdoor collapse of the Negra Muerta Caldera and motion on the Olacapato-El Toro Fault Zone, southern Central Andes. International Journal of Earth Science 95, 529–541. https://doi.org/10.1007/s00531-005-0042-x.

Rango, T., Vengosh, A., Dwyer, G., Bianchini, G., 2013. Mobilization of arsenic and other naturally occurring contaminants in groundwater of the main ethiopian rift aquifers. Water Res. 47, 5801–5818. https://doi.org/10.1016/j.watres.2013.07.002.

Robertson, F.N., 1991. Geochemistry of ground water in alluvial basins of Arizona and adjacent parts of Nevada, New Mexico, and California. In: U.S. Geological Survey Professional Paper 1406-C. https://doi.org/10.3133/pp1406C.

Robidoux, P., Rizzo, A.L., Aguilera, F., Aiuppa, A., Artale, M., Liuzzo, M., Nazzari, M., Zummo, F., 2020. Petrological and noble gas features of Lascar and Lastarria volcanoes (Chile): inferences on plumbing systems and mantle characteristics. Lithos 370-371 (105615). https://doi.org/10.1016/j.lithos.2020.105615.

Rodríguez, G.A., Bierlein, F.P., 2002. The Minas Azules deposit—an example of orogenic lode gold mineralization in the Sierra de Rinconada, northern Argentina. Int. Geol. Rev. 44, 1053–1067. https://doi.org/10.2747/0020-6814.44.11.1053.

Rodríguez, G.A., Azevedo, D., Coira, B., Brodie, C., 2001. Mineralizaciones auríferas en sedimentitas ordovícicas de la sierra de Rinconada (Jujuy-Argentina): implicancias para la exploración minera. Rev. Geológica Chile 28, 47–66. https://doi.org/10.4067/S0716-02082001000100003.

Rollinson, H.R., Pease, V., 2021. Using Geochemical Data: To Understand Geological Processes, 2nd ed. Cambridge University Press, p. 346.

Rudnick, R.L., Gao, S., 2005. Composition of the Continental Crust. In: Celo, V. (Ed.), The Crust. Elsevier, Amsterdam-San Diego-Oxford-London, pp. 1–64.

Rudnick, R.L., Gao, S., 2014. Composition of the continental crust. In: Holland, Heinrich D., Turekian, Karl K. (Eds.), Treatise on Geochemistry, Second edition. Elsevier, pp. 1–51. https://doi.org/10.1016/B978-0-08-095975-7.00301-6.

Ruggieri, F., Fernández-Turiel, J.L., Saavedra, J., Gimeno, D., Polanco, E., Naranjo, J.A., 2011. Environmental geochemistry of recent volcanic ashes from the Southern Andes. Environ. Chem. 8, 236–247. https://doi.org/10.1071/EN10097.

Ruggieri, F., Fernandez-Turiel, J.L., Saavedra, J., Gimeno, D., Polanco, E., Amigo, A., Galindo, G., Caselli, A., 2012. Contribution of volcanic ashes to the regional geochemical balance: the 2008 eruption of Chaitén volcano, Southern Chile. Sci. Total Environ. 425, 75–88. https://doi.org/10.1016/j.scitotenv.2012.03.011.

Salado Paz, N., Petrinovic, I., Do Campo, M., Brod, J.A., Nieto, F., da Silva Souza, V., Wemmer, K., Payrola, P., Ventura, R., 2018. Mineralogy, structural control and age of the Incachule Sb epithermal veins, the Cerro Aguas Calientes collapse caldera, Central Puna. J. S. Am. Earth Sci. 82, 239–260. https://doi.org/10.1016/j.jsames.2017.07.002.

Sanci, R., Panarello, H.O., Gozalvez, M.R., 2020. Environmental isotopes as tracers of mining activities and natural processes: a case study of San Antonio de los Cobres River Basin, Puna Argentina. J. Geochem. Explor. 213, 106517 https://doi.org/10.1016/j.gexplo.2020.106517.

Sarbas, B., 2008. The GEOROC Database as part of a growing Geoinformatics Network. Geoinformatics 42–43. http://georoc.mpch-mainz.gwdg.de/georoc/ (last assessed January 2022).

Seggiaro, R.E., Guzmán, S.R., Martí, J., 2019. Dynamics of caldera collapse during the Coranzulí eruption (6.6 Ma)(Central Andes, Argentina). J. Volcanol. Geotherm. Res. 374, 1–12. https://doi.org/10.1016/j.jvolgeores.2019.02.003.

Sigurdsson, H., Houghton, B., McNutt, S., Rymer, H., Stix, J. (Eds.)., 2015. The Encyclopedia of Volcanoes. Elsevier (1417 p).

Simon, A.C., Pettke, T., Candela, P.A., Piccoli, P.M., Heinrich, C.A., 2007. The partitioning behavior of as and au in S-free and S-bearing magmatic assemblages.

Geochim. Cosmochim. Acta 71, 1764–1782. https://doi.org/10.1016/j.gca.2007.01.005.
Smedley, P.L., Kinniburgh, D.G., 2002. A review of the source, behaviour and distribution of arsenic in natural waters. Appl. Geochem. 17, 517–568. https://doi.org/10.1016/S0883-2927(02)00018-5.
Smedley, P.L., Nicolli, H.B., Macdonald, D.M.J., Barros, A.J., Tullio, J.O., 2002. Hydrogeochemistry of arsenic and other inorganic constituents in groundwaters from La Pampa, Argentina. Appl. Geochem. 17, 259–284. https://doi.org/10.1016/S0883-2927(01)00082-8.
Smith, I.E.M., Németh, K., 2017. Source to surface model of monogenetic volcanism: a critical review. Geological Society, London, Special Publications 446, 1–28. https://doi.org/10.1144/SP446.14.
Soler, M., Caffe, P., Coira, B., Onoe, A., Kay, S.M., 2007. Geology of the Vilama caldera: a new interpretation of a large-scale explosive event in the Central Andean Plateau during the Upper Miocene. J. Volcanol. Geotherm. Res. 164, 27–53. https://doi.org/10.1016/j.jvolgeores.2007.04.002.
Stern, C.R., 2004. Active Andean volcanism: its geologic and tectonic setting. Rev. Geol. Chile 31, 161–206. https://doi.org/10.4067/S0716-02082004000200001.
Sulpizio, R., Dellino, P., Doronzo, D.M., Sarocchi, D., 2014. Pyroclastic density currents: state of the art and perspectives. J. Volcanol. Geotherm. Res. 283, 36–65. https://doi.org/10.1016/j.jvolgeores.2014.06.014.
Tapia, J., Murray, J., Ormachea, M., Tirado, N., Nordstrom, D.K., 2019. Origin, distribution, and geochemistry of arsenic in the Altiplano-Puna plateau of Argentina, Bolivia, Chile, and Perú. Sci. Total Environ. 678, 309–325. https://doi.org/10.1016/j.scitotenv.2019.04.084.
Tapia, J., Schneider, B., Inostroza, M., Álvarez-Amado, F., Luque, J.A., Aguilera, F., Parra, S., Bravo., M., 2021. Naturally elevated arsenic in the Altiplano-Puna, Chile and the link to recent (Mio-Pliocene to Quaternary) volcanic activity, high crustal thicknesses, and geological structures. J. S. Am. Earth Sci. 105, 102905 https://doi.org/10.1016/j.jsames.2020.102905.
Tapia, J., Mukherjee, A., Rodríguez, M.P., Murray, J., Bhattacharya, P., 2022. Role of tectonics and climate on elevated arsenic in fluvial systems: Insights from surface water and sediments along regional transects of Chile. Environ. Pollut. 314, 120151 https://doi.org/10.1016/j.envpol.2022.120151.
Taussi, M., Godoy, B., Piscaglia, F., Morata, D., Agostini, S., Le Roux, P., González-Maurel, O., Gallmeyer, G., Menzies, A., Renzulli, A., 2019. The upper crustal magma plumbing system of the Pleistocene Apacheta-Aguilucho Volcanic complex area (Altiplano-Puna, northern Chile) as inferred from the erupted lavas and their enclaves. J. Volcanol. Geotherm. Res. 373, 179–198. https://doi.org/10.1016/j.jvolgeores.2019.01.021.
Torres, I., Németh, K., Ureta, G., Aguilera, F., 2021. Characterization, origin, and evolution of one of the most eroded mafic monogenetic fields within the Central Andes: the case of El País lava flow field, northern Chile. J. S. Am. Earth Sci. 105, 102942 https://doi.org/10.1016/j.jsames.2020.102942.
Ureta, G., Aguilera, F., Nemeth, K., Inostroza, M., Gonzalez, C., Zimmer, M., Menzies, A., 2020a. Transition from small-volume ephemeral lava emission to explosive hydrovolcanism: the case of Cerro Tujle maar, northern Chile. J. S. Am. Earth Sci. 104, 102885 https://doi.org/10.1016/j.jsames.2020.102885.
Ureta, G., Németh, K., Aguilera, F., Vilches, M., Aguilera, M., Torres, I., Sepúlveda, J.P., Scheinost, A., González, R., 2020b. An Overview of the Mafic and Felsic Monogenetic Neogene to Quaternary Volcanism in the Central Andes, Northern Chile (18-28°Lat.S). In (Ed.), Updates in Volcanology - Transdisciplinary Nature of Volcano Science. IntechOpen. https://doi.org/10.5772/intechopen.93959.
Ureta, G., Nemeth, K., Aguilera, F., Zimmer, M., Menzies, A., 2021. A window on mantle-derived magmas within the Central Andes: Eruption style transitions at Cerro Overo maar and La Albóndiga lava dome, northern Chile. Bull. Volcanol. 83 (19) https://doi.org/10.1007/s00445-021-01446-3.
USGS and SGBO (U.S. Geological Survey and Servicio Geológico de Bolivia), 1975. Geology and Mineral Resources of the Altiplano and Cordillera Occidental, Bolivia. With a section on Application of economic evaluations to deposit models, by Donald I. B. and Robert G. C (378 p).
Valentino, G.M., Stanzione, D., 2003. Source processes of the thermal waters from the Phlegraean Fields (Naples, Italy) by means of the study of selected minor and trace elements distribution. Chem. Geol. 194, 245–274. https://doi.org/10.1016/S0009-2541(02)00196-1.
Vandervoort, D.S., Jordan, T.E., Zeitler, P.K., Alonso, R.N., 1995. Chronology of internal drainage development and uplift, southern Puna plateau, argentine Central Andes. Geology 23, 145–148. https://doi.org/10.1130/0091-7613(1995)023b0145:COIDDAN2.3.CO;2.
Welch, A.H., Lico, M.S., Hughesa, J.L., 1988. Arsenic 1n Ground Water of the Western United States. Groundwater 26 (3), 333–347. https://doi.org/10.1111/j.1745-6584.1988.tb00397.x.
Williams-Jones, A.E., Heinrich, C.A., 2005. 100th Anniversary special Paper: Vapor Transport of Metals and the Formation of Magmatic-Hydrothermal Ore Deposits. Econ. Geol. 100, 1287–1312. https://doi.org/10.2113/gsecongeo.100.7.1287.
World Health Organization (WHO), 2022. Guidelines for Drinking-Water Quality: Fourth Edition Incorporating the First and Second Addenda. Geneva. Licence: CC BY-NC-SA 3.0 IGO.
Wörner, G., Mamani, M., Blum-Oeste, M., 2018. Magmatism in the Central Andes. Elements 14 (4), 237–244. https://doi.org/10.2138/gselements.14.4.237.
Yuan, X., Sobolev, S.V., Kind, R., 2002. Moho topography in the Central Andes and its geodynamic implications. Earth Planet. Sci. Lett. 199, 389–402. https://doi.org/10.1016/S0012-821X(02)00589-7.
Zajacz, Z., Halter, W.E., Pettke, T., Guillong, M., 2008. Determination of fluid/melt partition coefficients by LA-ICPMS analysis of co-existing fluid and silicate melt inclusions: Controls on element partitioning. Geochim. Cosmochim. Acta 72, 2169–2197. https://doi.org/10.1016/j.gca.2008.01.034.
Zandt, G., Leidig, M., Chmielowski, J., Baumont, D., Yuan, X., 2003. Seismic detection and characterization of the Altiplano-Puna magma body, Central Andes. Pure Appl. Geophys. 160, 789–807. https://doi.org/10.1007/PL00012557.
Zkeri, E., Aloupi, M., Gaganis, P., 2015. Natural Occurrence of Arsenic in Groundwater from Lesvos Island, Greece. Water Air Soil Pollut. 226 https://doi.org/10.1007/s11270-015-2542-z.
Zkeri, E., Aloupi, M., Gaganis, P., 2018. Seasonal and spatial variation of arsenic in groundwater in a rhyolithic volcanic area of Lesvos Island, Greece. Environmental Monitoring and Assessment 190. https://doi.org/10.1007/s10661-017-6395-3.